ROCK PHYSICS STUDY AND ITS APPLICATION TO CHARACTERIZE MENGGALA RESERVOIR IN MALACCA STRAIT PSC

THESIS

By:
N A S L I N
0706172014

PHYSICS GRADUATE PROGRAM
FACULTY OF MATHEMATIC AND NATURAL SCIENCE
JAKARTA
2009

APPROVAL PAGE

Thesis submitted by

Name : N a s l i n

NPM : 0706172014

Study Program : Reservoir Geophysics

Thesis title : Rock Physics Study and Its Application to Characterize Menggala Reservoir in Malacca Strait PSC

Has been approved by the committee member and accepted in partial fulfillment of the requirement for the Degree of Master of Science in Reservoir Geophysics, Faculty of Mathematics and Natural Sciences, University of Indonesia.

Supervisor,

Prof. Dr. Suprajitno Munadi
NIP. 100 003 427

Examiners:

Dr. Abdul Haris Dr. Waluyo Dr. Ricky Adi Wibowo

Chairman,

Dr. Dedi Suyanto
NIP. 130 935 271

Defense date: **23rd May 2009**

ABSTRACT

A Rock physics study has been applied to guide interpretation and delineation of Menggala reservoir distribution in the DEFI field. Using rock physics, we can extrapolate the well data to geologically plausible conditions that might exist away from the well, exploring how the seismic signatures might change. The field to be investigated is located in the Malacca strait PSC, Central Sumatra Basin – Indonesia. In this research, the methodology consists of two phase: selecting the rock physics template that is consistent with the well log data and applying the user defined Rock Physics template to characterize reservoir distribution in the seismic data. An initial review of the data shows that it is reasonable quality and fits previously identified theoretical models, by using crossplot analysis. The result shows we can potentially distinguish rock physics of Menggala reservoir to delineate gas sand and potential porous sand distribution at the level of selected interval and finally generate a prospective undrilled area within DEFI field.

ABSTRAK

Studi tentang fisika batuan telah diterapkan dalam penelitian ini untuk memandu interpretasi dan deliniasi penyebaran reservoar Menggala di lapangan DEFI. Dengan studi fisika batuan, kita bisa mengekstrapolasi data data yang diperoleh dari sumur pemboran terhadap model geologi yang digambarkan melalui inversi data seismik. Lapangan yang akan diinvestigasi terletak di Blok Selat Malaka, Cekungan Sumatra Tengah - Indonesia. Dalam penelitian ini, metodologi yang digunakan terdiri dari dua tahap: pertama, mengenerasi model fiska batuan yang konsisten dari data log sumur, dan kedua, menerapkan model fisika batuan tersebut untuk memetakan penyebaran reservoar dari inversi data seismik. Hipotesis awal dengan menggunakan *crossplot analysis* menunjukkan bahwa data sumur yang digunakan mempunyai sensitifitas yang memadai terhadap sifat fisis batuan sesuai dengan model teoritis. Dan hasil akhir penelitian membuktikan bahwa analisis fisika batuan dapat mengkarakterisasi reservoar Menggala dengan menunjukkan potensi keberadaan fluida gas dan tingkat porositas batuan yang berimplikasi untuk pemetaan penyebaran potensi hidrokaron dan prospek pengeboran di lapangan DEFI.

FOREWORD

This thesis is the result of the hard-work process for my education at the University of Indonesia (UI). It was born through the process of self-precipitate, learning by doing, valuable discussing, consistency of thinking and serve in writing. I learned discipline to finish this thesis on time without ignoring the quality and maturity in learning.

I realize that my thesis needs much improvement. I also understand this may not satisfy some parties who related to the study. Therefore I apologize for all mistakes and confusions that may be found in this writing. As human being, I would like to express my gratitude to Allah SWT for His hidayah and giving me health and convenience to accomplish my postgraduate study. In this opportunity, please let me appreciate many parties who have helped and supported the author in completing the study and writing this thesis:

- Prof. Dr. Suprayitno Munadi as my supervisor in the University, thanks for giving me the opportunity to be explained and lectured the knowledge, and thanks for the scientific advices which contributed to the development of this thesis.
- As part of the G&G study was carried out at the Kondur Petroleum SA, I would like to thank all colleagues and management for providing the data and permitting to publish this study. I would like to thank also to all the people in the Exploration department for helping me in data processing.
- My classmate in University of Indonesia for valuable discussions and encouragement, giving me the wonderful time in the last two years as postgraduate student.
- And finally, the important part in the accomplishment of this thesis is Defi Arfianti, my beloved wife. Her sincere to accompany me in the joy and sadness, is a priceless treasure that coloring my life, present and future. Not forgotten, I bent on my knee to honor my beloved mother who never falls to be the sun in my 30 years life. For these two great women, I dedicate my thesis.

Jakarta, 31st May 2009

Table of Contents

Rock physics..., Naslin, FMIPA UI, 2009

Table of Figures

Rock physics..., Naslin, FMIPA UI, 2009

Rock physics..., Naslin, FMIPA UI, 2009

Rock physics..., Naslin, FMIPA UI, 2009

Chapter One:
INTRODUCTION

1.1. Background

Over the past few decades, the advances in rock physics theories have far outfaced our ability to make use of them in seismic interpretation. Using rock physics analysis of log data, the sensitivity rock physics parameters can be selected as indicators to differentiate fluid and lithology, which can be constrained and calibrated by log data. In this study, we show how rock physics techniques combined with seismic simultaneous inversion can be used to characterize reservoir and map the pore fluids distribution. The methods will be applied to Menggala formation in the DEFI field, in Malacca strait PSC - Central Sumatra Basin. The geological setting is a tertiary braided meandering system with heterogeneous sand and fluid distributions. Conventional seismic reservoir characterization may be very uncertain in these depositional environments. Linking 3D seismic imagery with rock physics properties of different facies and pore fluids can provide a supplement strategy for improved quantitative interpretation of seismic data.

Several studies have been performed since 1984 to 2004 in order to have a better understanding of Menggala formation. However none of the result produces a clear solid strategy that can be implemented to develop Menggala formation to fulfill the need to increase gas production and deliverability. Most of previous study was focused to understand the depositional and structural setting of Menggala formation. Even more than fifty wells has been drilled penetrating this formation but many of the well production result are not encouraging, excluding DEFI structure in the middle part of Malacca Strait PSC. This study result will show how this method can be used to further promote Menggala formation as a primary exploration target, with the DEFI field as a working example where rock physics technique is applicable to define reservoir properties and improved interpretation away to the neighbor field by seismic inversion.

1.2. Thesis Objective

The objective of this study is to obtain reliable quantitative estimates, with their uncertainties, for Menggala exploration play in the area of Malacca Strait PSC, Central Sumatra Basin. This study is divided into two phases: first phase focusing on Rock physics analysis based on well log data and the second phase is focused on seismic data analysis by performing simultaneous inversion method.

The first phase is aimed to generate and validate rock physics model to local condition of Menggala reservoir and assess the seismic detect ability of observed porosity and fluid variations. The second phase is aimed to obtain acoustic and elastic parameter from seismic data for underlying in the rock physics model resulted from first phase. The link between first phase and second phase will be a guide to map reservoir distribution of Menggala formation.

This study is partially to fulfill the requirements for the master degree of science in Reservoir Geophysics postgraduate program, Faculty of Mathematics and Natural Sciences, Department of Physics, University of Indonesia

1.3. Area

The research area is located in the middle part of EMP Malacca strait PSC operation area in Central Sumatra Basin, Indonesia (figure 1.1). Well data which are used as key well in this study is located in the DEFI field which is producing gas from Menggala Formation. This study is a part of Near Field Exploration project to support DEFI field development

1.4. Hypothesis

An initial review of the data shows that it is reasonable quality and fits identified theoretical models (figure 1.2). These crossplots tell us the data trends behavior in terms of seismic detectability. The two main scenarios then will be analyzed and mapped: what happens with variable fluid content and what happens with porosity variations. The simulation of fluid and porosity substitution increase the confidence that acoustic and elastic parameters are sensitive to the Menggala reservoir behavior then we may predict quantitatively reservoir character (such as porosity, shale volume, and saturation) away from the well

Rock physics..., Naslin, FMIPA UI, 2009

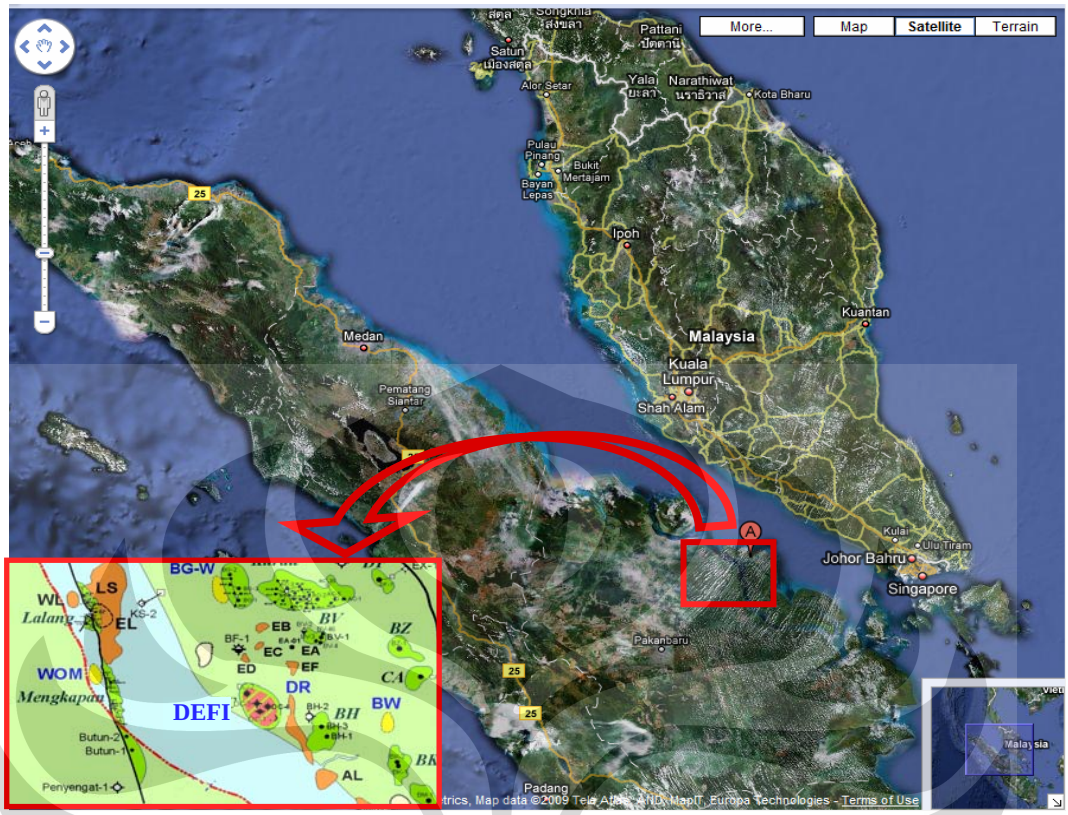

Figure 1.1. Map showing the area of the thesis in Malacca Strait Block

.

1.5. Implication of the Research

The integration of well log based rock physics analysis and modeling to the seismic inversion feasibility response, will guide the interpretation and give an ever increasing confidence that the model can be used to drive the static Menggala reservoir model in the DEFI field. This study is potentially resolves ambiguities between different types of porosity and fluid scenario and determines the porous gas sands reservoir distribution through seismic data based on rock physics template which is validated from well log data. In order to further explore Menggala reservoir and develop DEFI field in the Malacca Strait block, a prospective drillable area could be generated based on integration of reservoir distribution map and geological structure map. This study result may also be implemented as complementary technique to expand Menggala reservoir exploration to neighbor field outside study area.

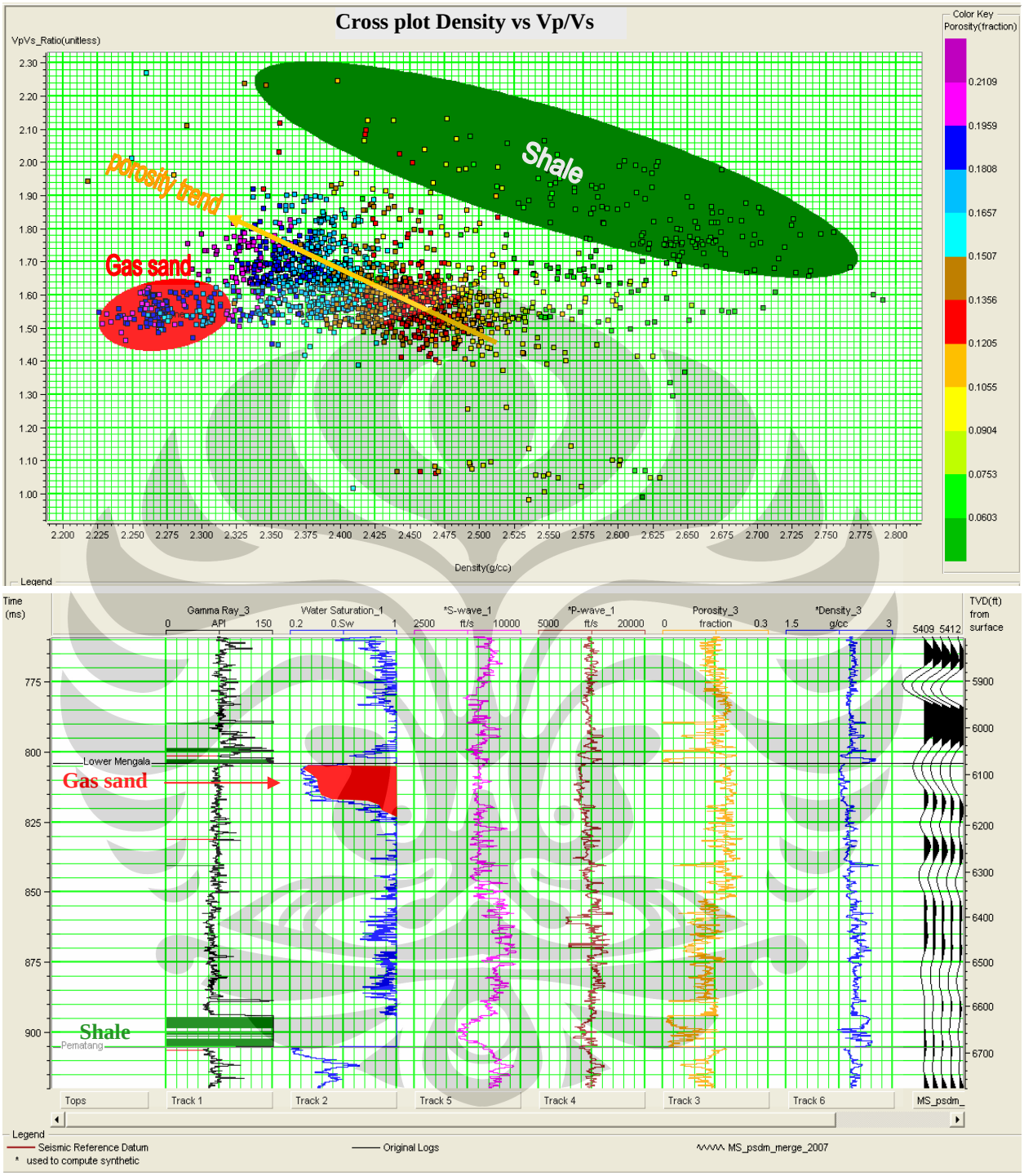

Figure 1.2. Data sensitivity analysis using rock physics parameter cross plot

Chapter Two:
BACKGROUND THEORY

2.1. Regional Geology and Generalized Petroleum System

DEFI structure is regionally located in the shoulder of Bengkalis Trough, formed as a four way dip closure as a result of reactivation an antithetic fault on the eastern margin of the Bengkalis Trough during Early Oligocene to Late Miocene orogeny or during the earliest part of Lower Menggala deposition. The Bengkalis Through is a half graben that is bounded to the west by a large border fault and flexural margin to the east. This basin is oriented approximately north south and 40-50 km long and 15-25 km wide (figure 2.1). This half graben geometry is a result of regional extensional in the Eocene to Oligocene (50-26 Ma) as a response to the major tectonic event that centered on the collision of India with southern Asia (Lambiase, 1997).

The stratigraphy of DEFI area showed in Figure 2.2 consists of formation from basement through Minas formation, which is inferred from all DEFI- wells. Regionally from bottom to top, DEFI stratigraphy depositional can be setting summarized as no marine system, transition system, delta system, marine system, and then starts again with non marine sediment in Minas formation

Based on GR log pattern analysis the sedimentation during Menggala time is a fluvial setting from alluvial fan too more meandering stream at Transition time. In this area, The Menggala Formation is divided into the Upper and Lower Members on lithological aspects. The Upper Menggala Member characterized by interbedded sand in log response and the Lower Menggala Member characterized by massive sand in log response (figure 2.3).

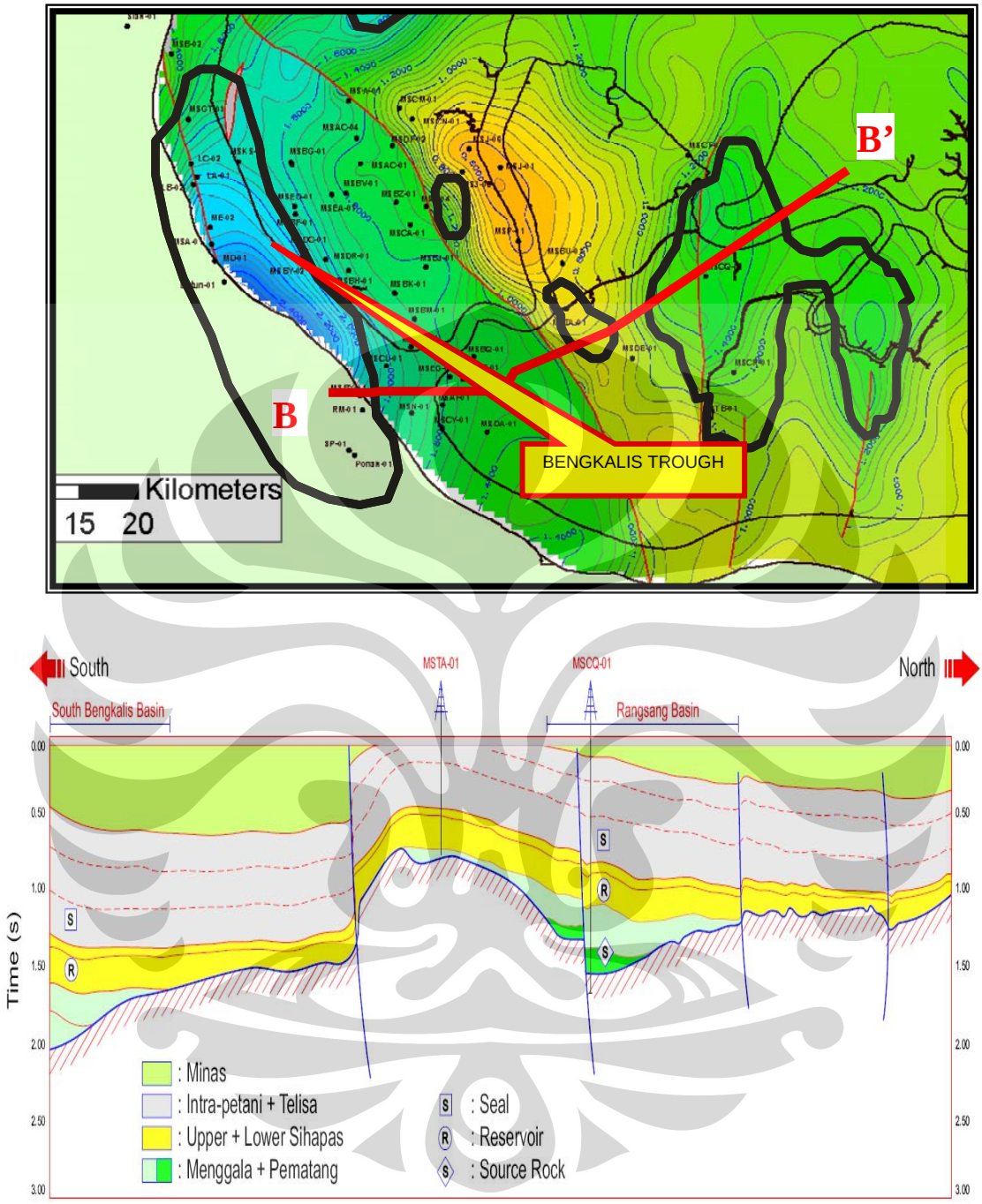

Figure 2.1. Structure map of Bengkalis Through with N-S cross section to show geological feature of the sub basin

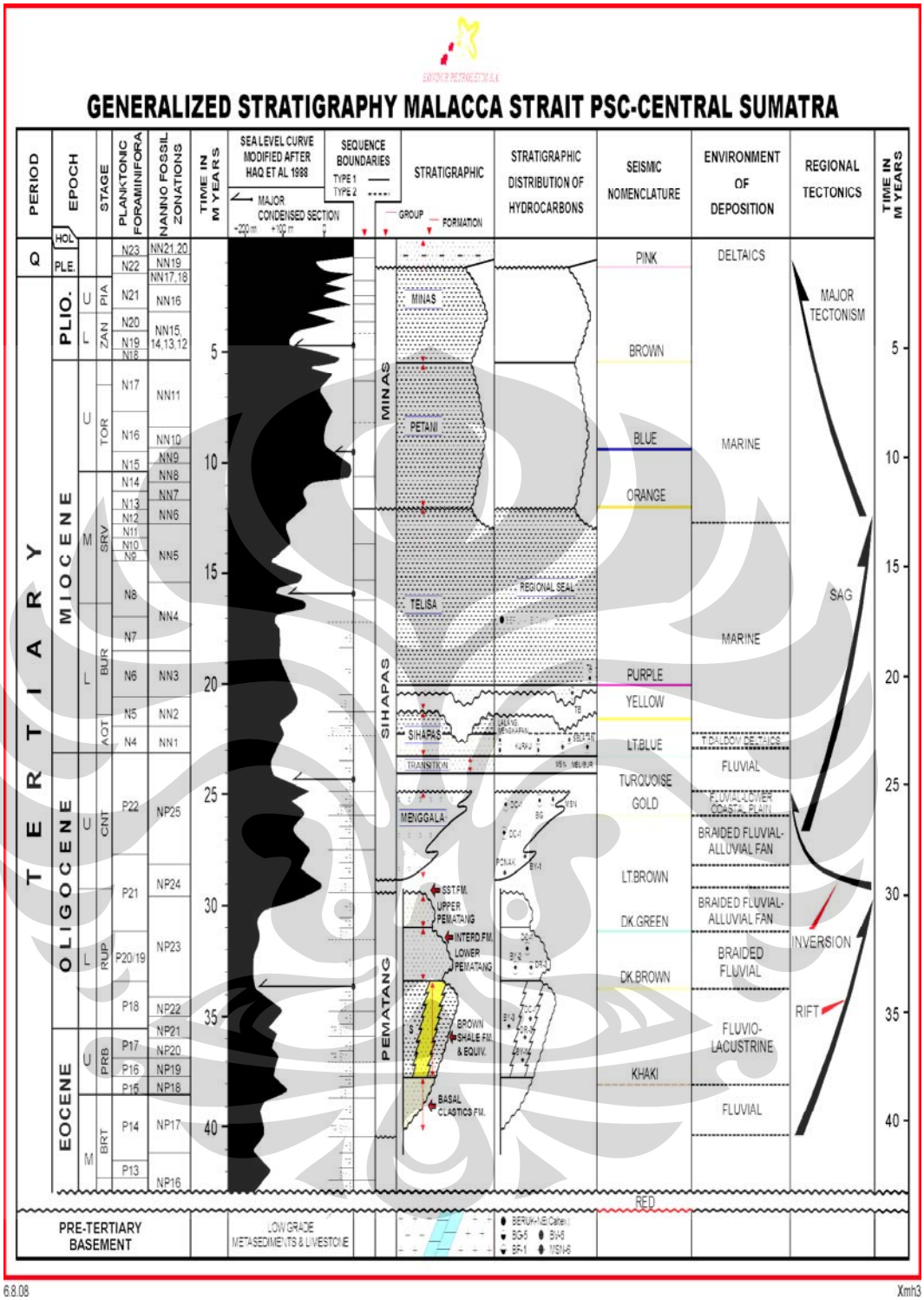

Figure 2.2 Updated general stratigraphy of DEFI Structure – Bengkalis Through

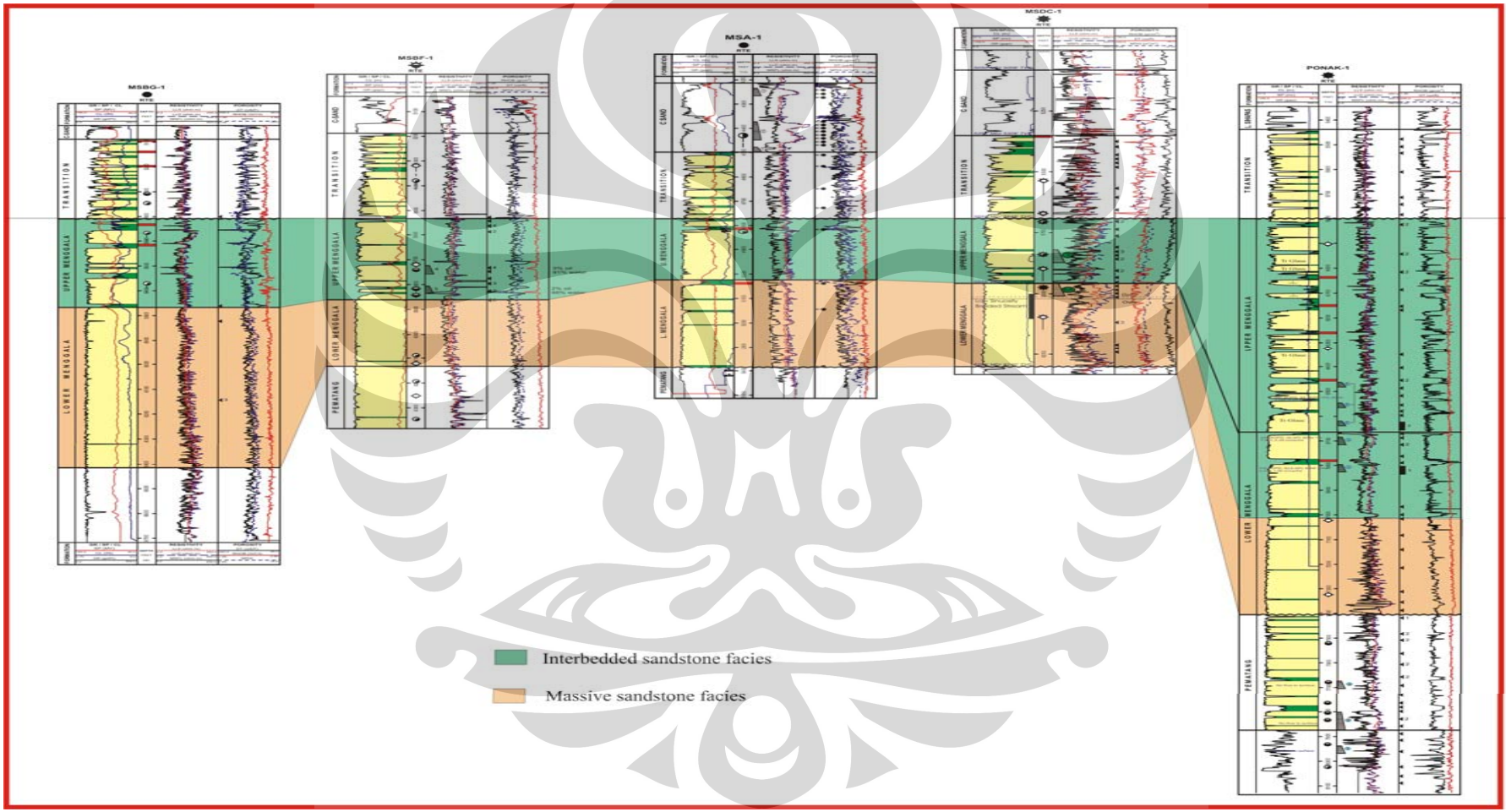

Figure 2.3. Log correlation displaying Upper Menggala member and Lower Menggala member

In the Bengkalis Trough, the interbedded mudstones and shales comprise the intraformational seals. The intraformational shale in Transition-Menggala Formation can be act as a intraformational seal or cap rock for trapping hydrocarbon as observed in DEFI Field and Ponak/Selat Panjang Field (Petroselat PSC). Oil discoveries within the basin were initially attributed to sourcing from coals of the Sihapas Formation. However, the primary source rock is now considered to be lacustrine shales within the Pematang Brown Shale. The onset of oil generation and expulsion from the modeled Brown Shale interval is indicated to have occurred at end-Oligocene to earliest Miocene times and continues to the present day. The first gas generation is modeled to have occurred in the Late Miocene and continues to the present day in the deeper parts of the graben. The timing of migration of hydrocarbons related to the timing of trap formation is generally quite favorable. Individual structure in Menggala may formed in different time migration stage, but basically categorized either from early to intermediate or to late oil generation time. The oldest (Late Oligocene) pre-dates expulsion whilst the Early-Mid Miocene and Late Miocene - Pleistocene traps are charged by hydrocarbons migrating throughout the Neogene.

Hydrocarbon trap in the DEFI field may be categorized by three type, they are stratigraphic, structural, and combination of structure and stratigraphic. The depositional setting of Menggala, which is Alluvial-Coastal plain deposit, may formed stratigraphic trap by geometry shape of the sandstones or by facies changes in lateral way. Complex structure evolution in this basin from Eocene time to Plio-Pleistocene may develop structural trap. In the DEFI Field, Menggala prospect is a low relief four way dip closure, both at Top of Menggala and Intra Menggala levels. The structures were formed as a result of structural inversion appears to have been developed during the Late Oligocene. It is inferred that an intraformational seal is going to be effective for trapping hydrocarbon at this level.

2.2. Reservoir Properties

As mentioned above, The Menggala formation was deposited in a fluvial-alluvial environment, producing reservoir normally consists of coarse

conglomeratic sandstones with fair to good porosity and fair permeability. During tectonic activity and sedimentation buried from mid Oligocene to Plio-Pleistocene the reservoir characteristic may be reduce or increase.

The top Upper Menggala Member is corresponds to the turquise seismic horizon, on the wireline logs the pick coincides with marked increase velocity and density and decrease of GR and Neutron porosity. The sand consists of predominantly medium to coarse quartzitic sandstone and conglomerates with minor claystone interbeds in the lower part. The sandstone become conglomeratic in part and contains high proportion of kaolinitic matrix formed by alteration of feldspar. Porosity range between 10-16%, and permeability is low (less than 1 MD).

Top Lower Menggala Member was picked at the sharp contact between shaly sandstones interbedded with claystones and the underlying blocky clean sandstones. On seismic is corresponds to the gold seismic event, which is a moderately broad through which is followed by moderately broad peak on seismic data. The sands are massive conglomeratic quartz sandstones and interpreted as braided stream multistory channel or alluvial fan. Lower Menggala sand is the main reservoir in DEFI wells, contain 30-90 ft gas column and 25-30 ft column condensate. This sand was interpreted as multistory channel of braided river system based on conventional core in DEFI-1 and DEFI-2 well and logs curve. The log curve shows thick blocky sandstone, which has 300-350 ft thick. DST test in DEFI-1 well flowed 317 BPD condensate, 16380 MSCFGD gas, and 76 BWPD water (figure 2.4). The Lower Menggala sand is a main reservoir in the DEFI field. This sand classified as probable reservoir in DEFI-1 well.

The petrophysical data of DEFI field was taken from the summary of DEFI-1 well log analysis (Table 2-1). Kuat field has 2 gas zones in the Lower Menggala and Upper Menggala sandstones reservoirs. The oil bearing is only present in Lower Menggala as an oil rim with the thickness of 27 ft.

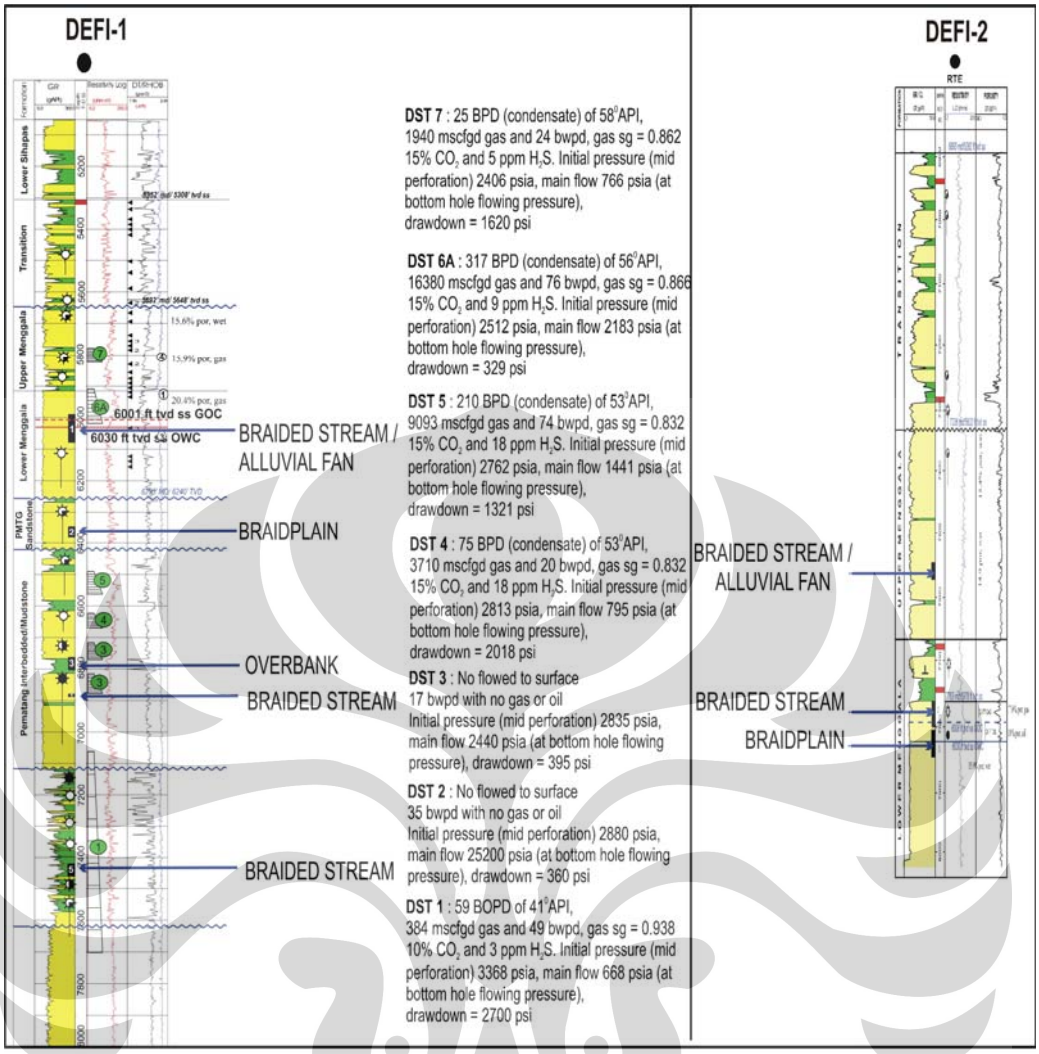

Figure 2.4. DST summary from DEFI-1 exploration well, prove gas and condensate contain in upper and lower Menggala formation

Table 2-1 : DEFI-1 Petrophysical Summary

Sand Name	Top (ft.BRT)	Base (ft.BRT)	Net Pay (ft)	Phie (%)	Sw (%)
Upper Menggala-Gas	5828	5860	26.5	15.23	64.6
Lower Menggala-Gas	5958	6050	90.5	16.24	41.29
		Total	**136.5**		

The reservoir properties and performance of the DEFI field are obtained from DST analysis of the DEFI-1 well. Seven (7) DSTs were conducted in MSDC-1 well commenced in January 1991, Two (2) of them (DST-6 to DST-7) represents the reservoir performance of Upper and Lower Menggala. DST-6 tested the Lower Menggala formation which have depth interval 5958-6060ft BRT. The following data is the summary of DST-6 during flowing period (Tabel 2-2)

Table 2-2 : DEFI-1 production test Summary.

Choke Size	1/64 inch	56/64	80/64	28/64	40/64
Duration	hours	5.5	1.5	3	3
WHFP	psig	1155	650	1910	1629
WHFT	deg.F	191	190	162	185
Gas Rate	mmscfpd	13.703	16.384	5.586	10.372
Oil/Condensate	bpd	303	317	213	274
Water Rate	bpd	132	75.8	57.8	102.8
GOR	scf/bbl	45,224	51,685	27,495	37,854
Water Cut	%	30	19	21	27
Gas Gravity	(air = 1.0)	0.864	0.866	0.822	0.85
API of Oil/Condensate	deg. API	56.7	55.9	55.4	56.9
Pwf @5935 ft.TVD	psia	2,220	2,168	2,416	2,338

2.3. Rock Physics

Rock physics is a technique that relates the geological properties (e.g. porosity, lithology, saturation) of a rock at certain physical conditions with the corresponding elastic and seismic properties (e.g. elastic modulus, velocity, impedance). The technique can be to predict the seismic properties from the geology or to predict geology from seismic observations vice versa (figure 2.5).

Rock physics modeling is frequently used in conjunction with well log data, either to help classify well log measurements or to predict geophysical logs based on geological measurements. An important task for rock physics analysis is to obtain proper physical parameters for indicating fluid and lithology from well log data. Generally three independent rock physics parameters can be extracted from well log and seismic data. They are density (ρ), P-wave velocity and S-wave velocity (Avseth et al, 2005). These three basics parameters can be used to derive several elastic parameters or their combinations that have different abilities for

discriminating fluid and lithology. Figure 2.6 is the example of Rock physics model application (known as RPT: Rock physics Template) to discriminate fluid and lithology in the deepwater area, Gulf of Mexico (Chi & Han, 2009)

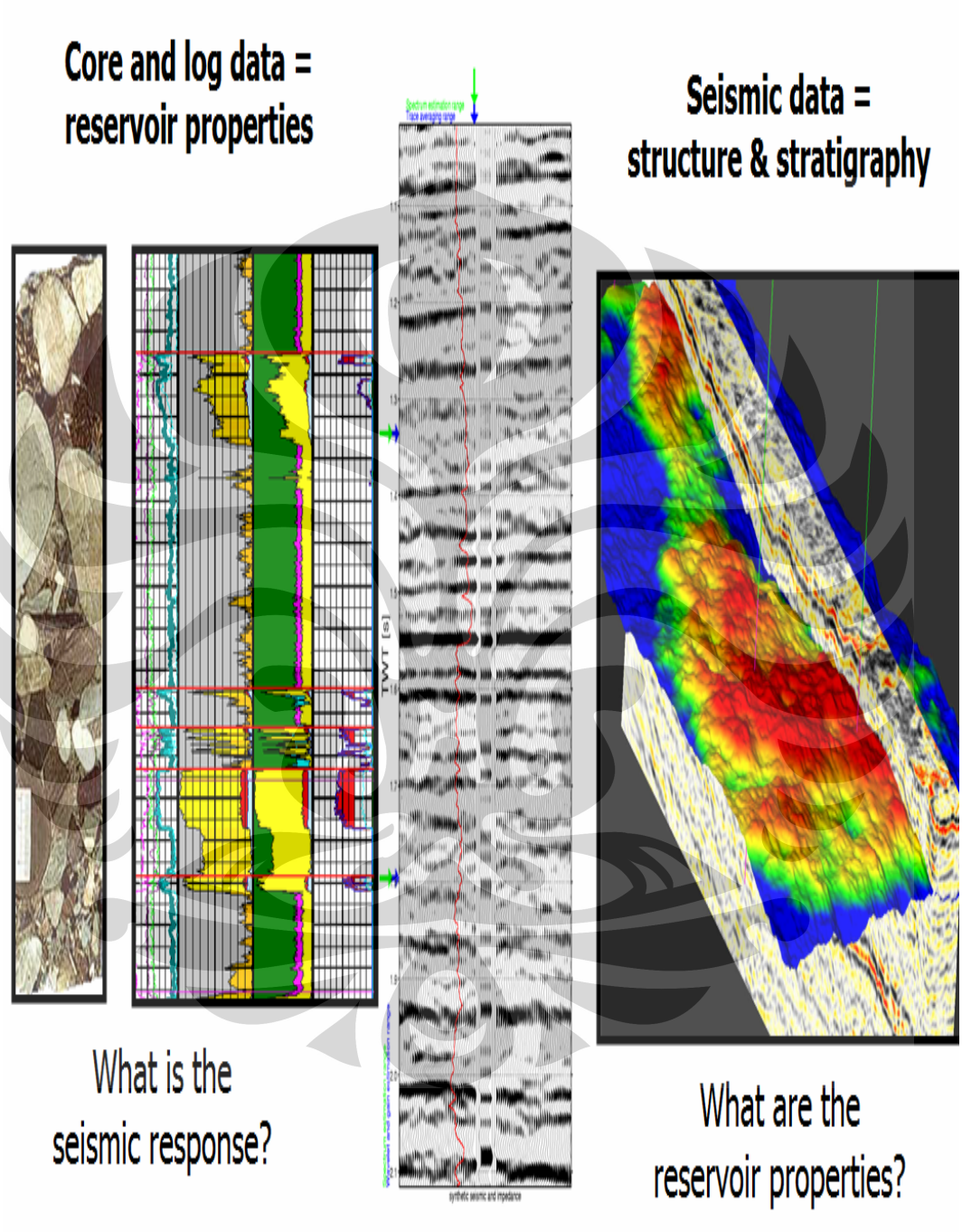

Figure 2.5. Rock Physics is the link between well log and seismic data to better understanding reservoir properties

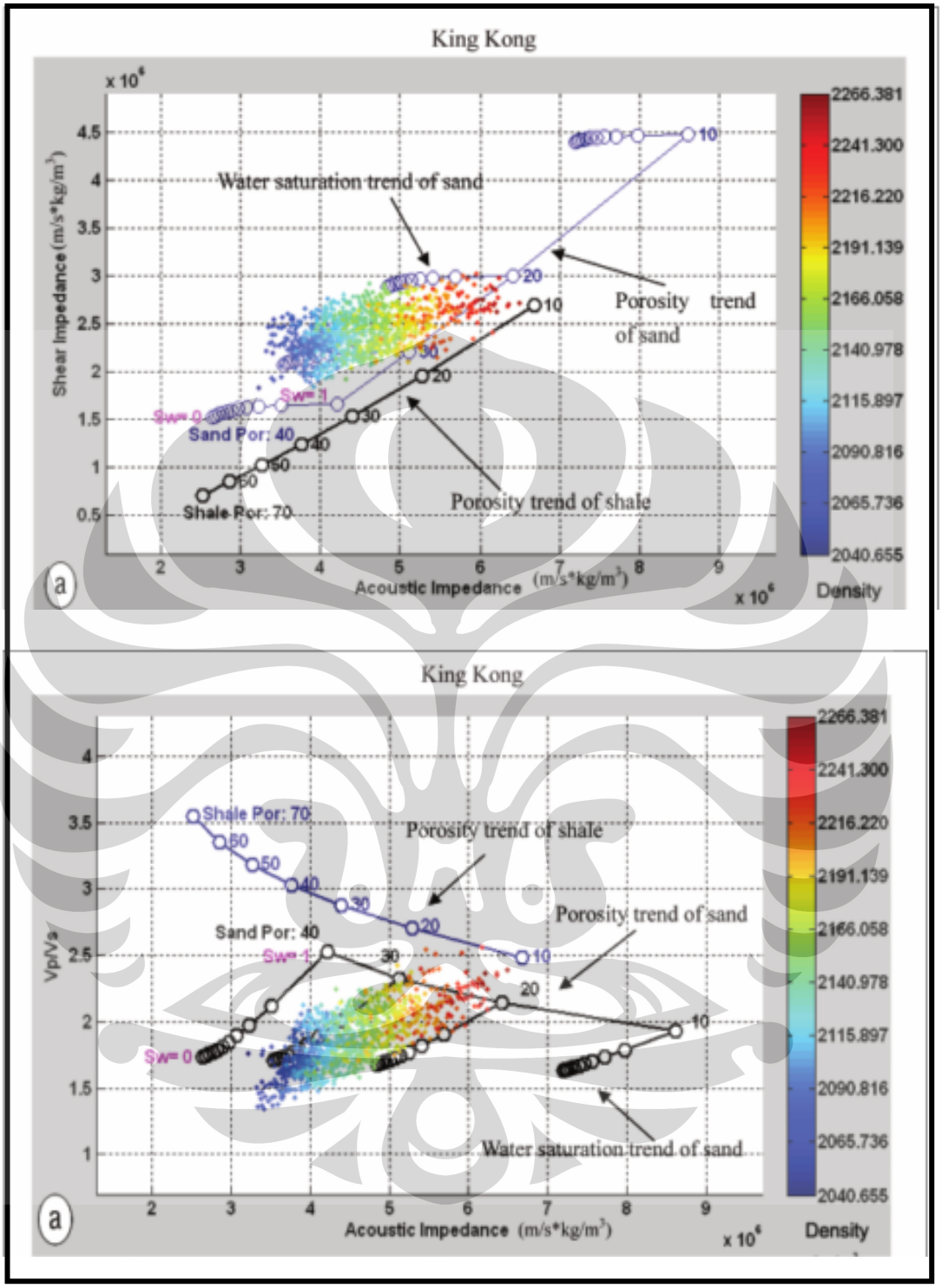

Figure 2.6. Rock Physics model applied in Gulf of Mexico, to differentiate fluid and lithology of reservoir studied (Chi & Han, 2009)

Rock physics models that relate velocity and impedance to porosity and mineralogy form a critical part of seismic analysis for porosity distribution and prediction. We can see later in this study how the porosity variation has a significant contribution to change elastic (seismic) parameters. Gassman (1951, in Avseth at al, 2005) has represented velocity-porosity relation in the form below:

$$\frac{1}{K_{rock}} = \frac{1}{K_{\min eral}} + \frac{\phi}{\tilde{\tilde{K}}_{\phi}} \qquad (2.1)$$

Where K_{rock}, $K_{\min eral}$, and $\tilde{\tilde{K}}_{\phi}$ are the bulk moduli of the saturated rock, the mineral and the saturated pore space, respectively, and ϕ is the porosity. Hence, we can see that the sensitivity of rock modulus (and velocity) to pore fluid changes depends directly on the ratio of pore space stiffness to porosity, $\tilde{\tilde{K}}_{\phi} / \phi$. Rocks that are relatively stiff have a small seismic sensitivity to pore fluids and rocks that are soft have a large sensitivity to pore fluids (Avseth et al, 2005). To more understand velocity-porosity relation, figure 2.7 shows the acoustic properties of sediments. The figure demonstrates P-wave velocity versus porosity for a variety of water-saturated sediments, ranging from ocean-bottom suspensions to consolidated sandstones. The Voigt and Reuss bounds, computed for mixtures of quartz and water, are shown for comparison. (Strictly speaking, the bounds describe the allowable range for elastic moduli. When the corresponding P- and S-wave velocities are derived from these moduli, it is common to refer to them as the "upper and lower bounds on velocity.")

What about Vs behavior in term of porosity trend? Next figure (2.8) show that porosity acts similarly enough on both Vp and Vs with gas-saturated rock velocity data superimposed. The gas and water-saturated data fall along two well-separated trends. We also see that clay tends to lower velocity, acts similarly enough on both V_P and Vs.

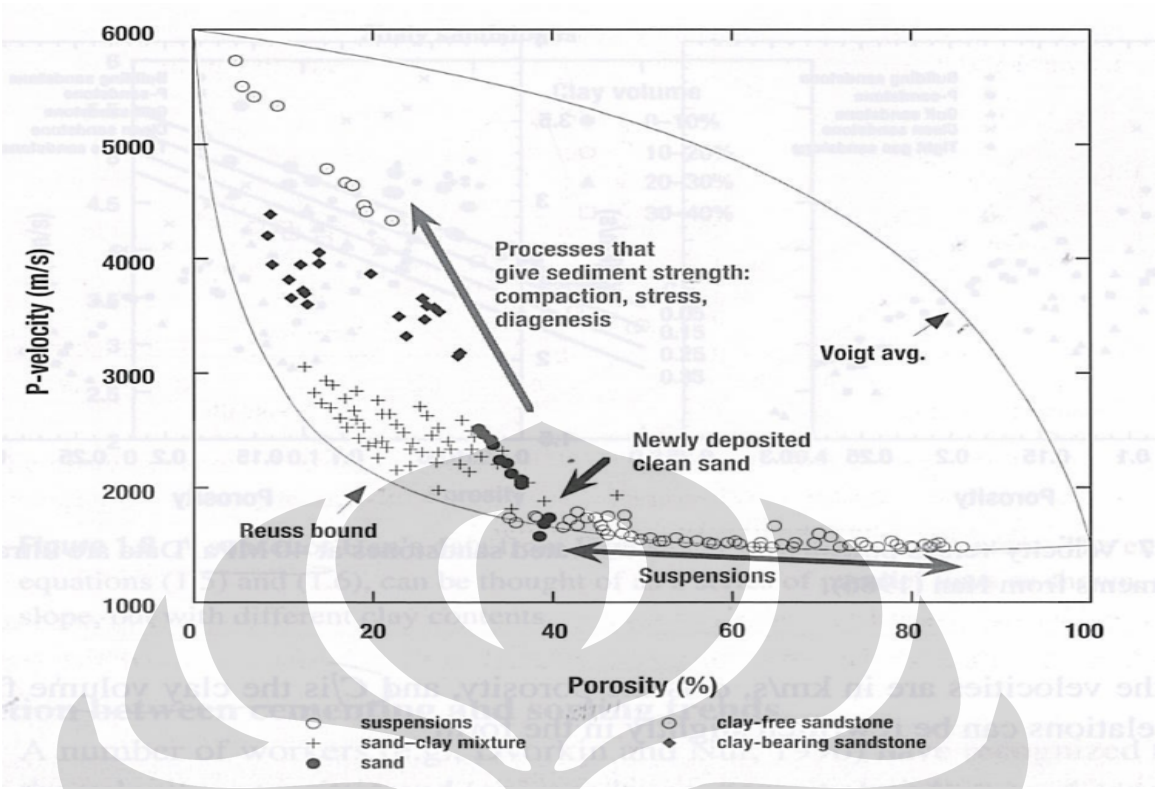

Figure 2.7 P-wave velocity versus porosity for a variety of water-saturated sediments, compared with the Voigt-Reuss bounds. Courtesy from Avseth et al, 2005

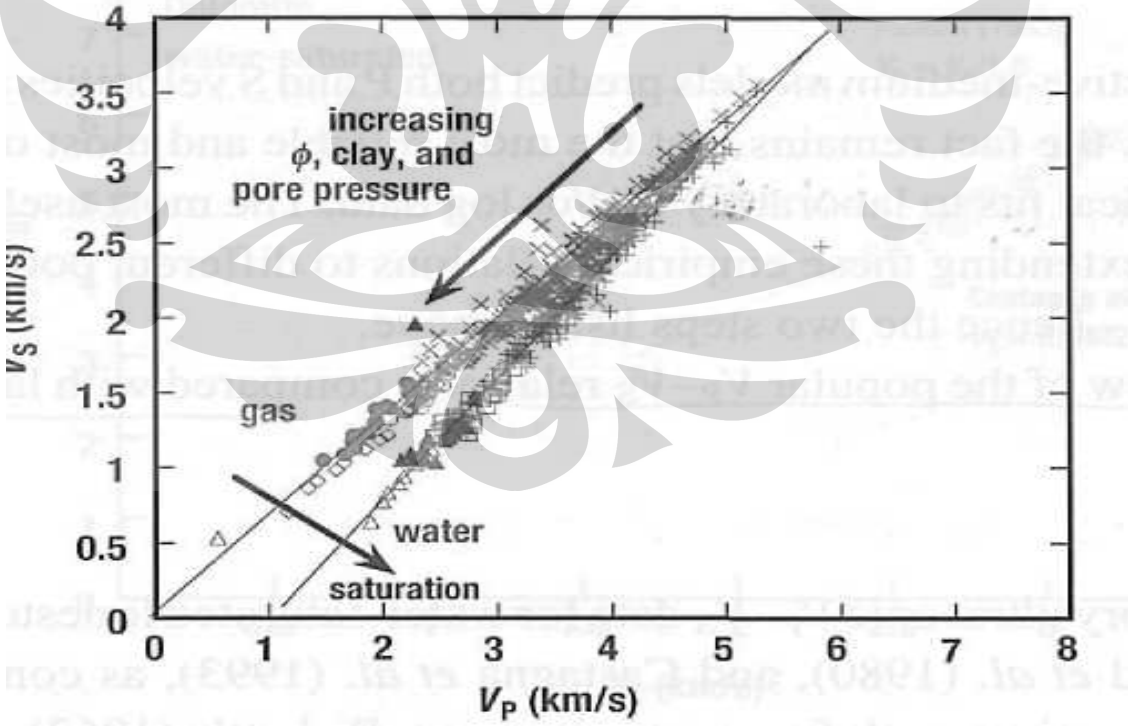

Figure 2.8 Plot of *Vs* vs. Vp for water-saturated and gas-saturated sandstones, with porosities of 4-40%, effective pressures 5-50 MPa, clay fraction 0-50%. Arrow shows direction of increasing porosity, clay, pore pressure. The trend of saturation is perpendicular to that for porosity, clay, pore pressure (Avseth et al, 2005)

For the fluid substitution problem, there are two fluid effects that must be considered: the change in rock bulk density, and the change in rock compressibility. The compressibility of a saturated rock can be expressed by the low frequency Gassmann theory (Gassmann, 1951) as:

$$K_{sat} = K_{frame} + \frac{\left(1 - \frac{K_{frame}}{K_{matrix}}\right)^2}{\frac{\phi}{K_{fl}} + \frac{(1-\phi)}{K_{matrix}} - \frac{K_{frame}}{K^2_{matrix}}} \qquad (2.2)$$

Where, K_{frame}, K_{matrix}, and K_{fl} are the bulk moduli of the saturated rock, porous rock frame (drained of any pore-filling fluid), mineral matrix, and pore fluid, respectively, and ϕ is porosity (as fraction). In the Gassmann formulation shear modulus is independent of the pore fluid and held constant during the fluid substitutions. Bulk modulus (K_{sat}) and shear modulus (μ) in turn can be estimated from the wireline log data (related to P-wave velocity V_p and S-wave velocity V_s) by rewriting equation as

$$K_{sat} = r\left(V_P^2 - \tfrac{4}{3}V_S^2\right)$$

and

$$\mu = \rho V_S^2 \qquad (2.3)$$

Where ρ is the bulk density given by $\rho = \phi\,\rho_{fluid} + (1- \Phi)\,\rho_{mineral}$

An example of fluid substitution effects on seismic signatures is shown in Figure 2.9 that well logs penetrating a Sandy turbidite sequence. Along with it (top right) are the corresponding normal incidence synthetics, assuming a 50Hz ricker wavelet. The initial logs showed an average water saturation of about 10% in the thick sand, with light oil of 35 API, GOR of 200 Sm^3/Sm^3. It was applied Gassmann fluid substitution, increasing the water saturation to 90%, with brine salinity of 30,000 ppm. The predicted result are shown at the bottom of the picture. On the left, we see that replacing light oil with water increases the density and P-wave velocity in the sand. The impedance increases by about 8 %. The

synthetics show that the fluid substitution results in both amplitude changes and travel time pull up (earlier arrivals).

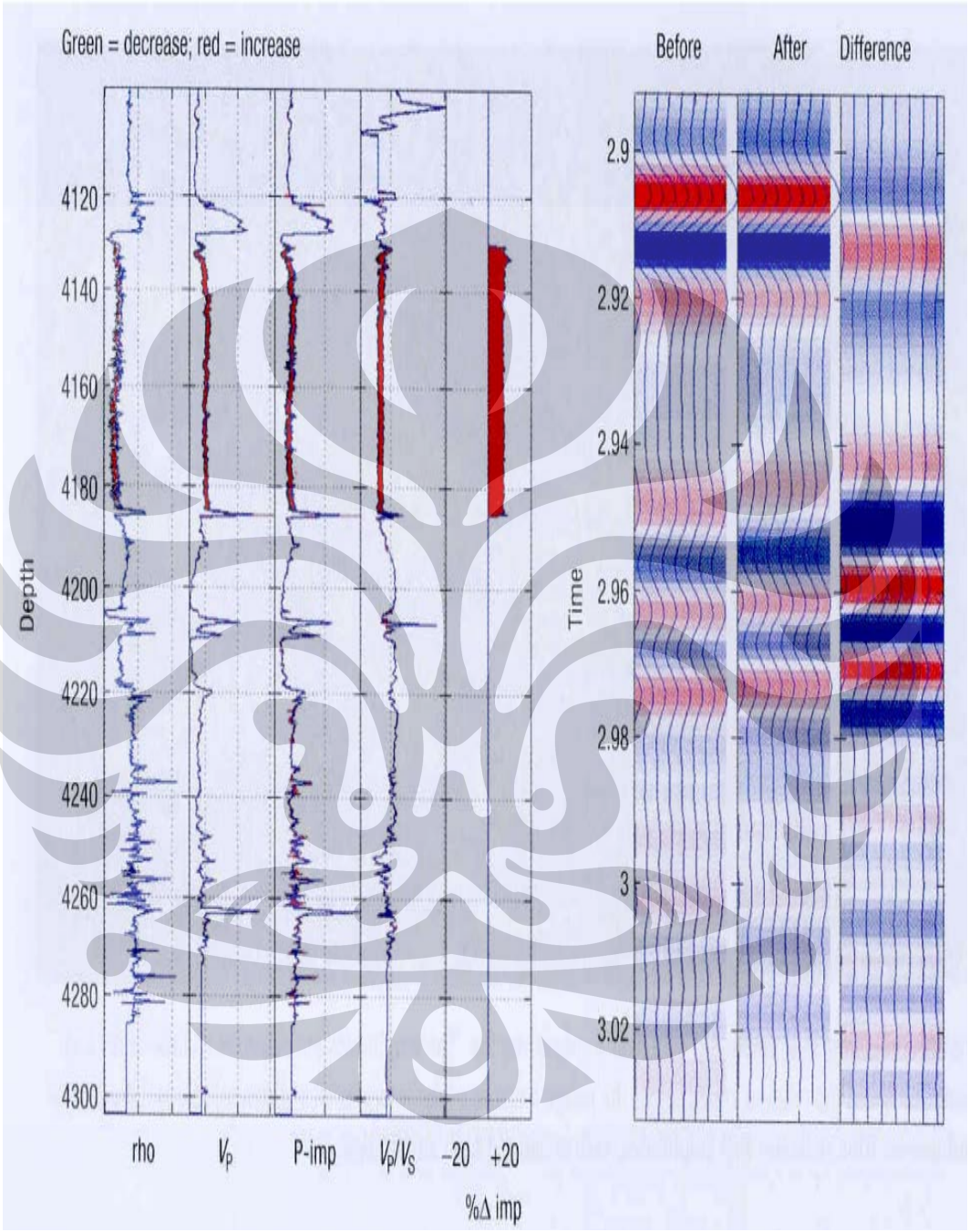

Figure 2.9. Logs penetrating a sandy turbidite sequence, increasing water saturation from 10 % to 90% increases density and V_p (left) and giving both amplitude and traveltime changes (right)

2.4. Simultaneous Seismic Inversion

Seismic inversion is a contrary of numerical modeling. In seismic exploration, numerical modeling is a technique to simulate geological feature yielding seismic trace, so as seismic inversion is a technique to retrieval the geological feature (Munadi, 2005). Numerical modeling, commonly known as a forward modeling and seismic inversion requires a knowledge of seismic wave behavior when propagate in porous media. The propagation of seismic wave in porous media containing fluid as function of petrophyiscal properties of rock was described previously in Rock physics section

In simultaneous inversion, some partial seismic angle stack is combined to obtain angle dependent quantities such as P-Impedance, S- Impedance and Vp/Vs ratio. However, the calculation of angle dependent provides synthetic seismic for each partial angle stack less precise than the synthetic seismic obtained directly from elastic inversion, such as information from seismic data is not entirely used in the calculation of the angle independent. Other problem is the actual frequency of partial stack that is used for the inversion, which far offset data contains low frequency due to attenuation and NMO (Normal Move Out) stretch. Problem appears when elastic Impedance combined in angle independent quantities because combining the data with the different frequency, create noise in the calculation of angle independent.

A contrary of the elastic impedance, in simultaneous inversion all seismic data inverted simultaneously for all independent angles (Ma, 2002). The advantage of this process is to stabilize the problem non-unique analysis of the inversion results and sensitive to noise. Simultaneous inversion using stack seismic data inputs from various angles (near, mid, and far) and then together be inverted with the wavelet estimated from each stack to obtain Vp, Vs, and density information.

Starting from the CDP gather, we apply the Aki-Richards equation (modified by Fatti et al, 1994) to get reflectivity:

$$R_{PP}(\theta) = c_1 R_P + c_2 R_S + c_3 R_D \qquad (2.4)$$

where

$$c_1 = 1 + \tan^2\theta$$
$$c_2 = -8\gamma^2 \sin^2\theta$$
$$c_3 = -\frac{1}{2}\tan^2\theta + 2\gamma^2 \sin^2\theta \qquad (2.5)$$
$$\gamma = \frac{V_S}{V_P}$$

and

$$R_P = \frac{1}{2}\left[\frac{\Delta V_P}{V_P} + \frac{\Delta\rho}{\rho}\right]$$
$$R_S = \frac{1}{2}\left[\frac{\Delta V_S}{V_S} + \frac{\Delta\rho}{\rho}\right] \qquad (2.6)$$
$$R_D = \frac{\Delta\rho}{\rho}$$

Where R_{pp} is total reflectivity, R_p is the P-wave reflectivity, R_s is S-wave reflectivity, R_d is density reflectivity, V_p is the P-wave velocity, V_s is S-wave velocity and ρ is the density. To transform equation from reflectivity to Impedance, we defined a new variable $L_p = \ln(Z_p)$, which is the normal log of the acoustic Impedance, Z_p.

$$R_P(i) = 1/2\left[L_P(i+1) - L_P(i)\right] \qquad (2.7)$$

Or written in the matrix as follows:

$$R_P = (1/2)DL_P$$

or

$$\begin{bmatrix} R_P(1) \\ R_P(2) \\ \vdots \\ R_P(N) \end{bmatrix} = \frac{1}{2}\begin{bmatrix} -1 & 1 & 0 & \cdots \\ 0 & -1 & 1 & 0 \\ 0 & 0 & -1 & 1 \\ 0 & 0 & 0 & \cdots \end{bmatrix}\begin{bmatrix} L_P(1) \\ L_P(2) \\ \vdots \\ L_P(N) \end{bmatrix} \qquad (2.8)$$

Then added wavelet effect in matrix equation:

$$T = WR_P$$

or
$$\begin{bmatrix} T(1) \\ T(2) \\ \vdots \\ T(N) \end{bmatrix} = \frac{1}{2}\begin{bmatrix} W_1 & 0 & 0 & \cdots \\ W_2 & W_1 & 0 & \cdots \\ W_3 & W_2 & W_1 & \cdots \\ 0 & W_3 & W_2 & \cdots \end{bmatrix}\begin{bmatrix} -1 & 1 & 0 & \cdots \\ 0 & -1 & 1 & 0 \\ 0 & 0 & -1 & 1 \\ 0 & 0 & 0 & \cdots \end{bmatrix}\begin{bmatrix} L_P(1) \\ L_P(2) \\ \vdots \\ L_P(N) \end{bmatrix} \qquad (2.9)$$

Where T is the seismic trace and W is the seismic wavelet. The same is done for the $L_s = \ln(Z_s)$ and $L_D = \ln(Z_D)$ where Z_s is the S-Impedance and Z_D is the density. Now Aki-Richards equation can be written as follows:

$$T(\theta) = (1/2)c_1 W(\theta) DL_P + (1/2)c_2 W(\theta) DL_S + c_3 W(\theta) DL_D \qquad (2.10)$$

In this case we model seismic trace, T on the θ angle as a function of Impedance and density. This equation is also possible for different wavelet with different angle.

To obtain P-Impedance, S-Impedance and density, we use the fact that the density and Impedance related to one another. We use the equation that is expected to represent the wet trend. We assume that the wet conditions can be modeled as the constant Vp/Vs ratio:

$$V_S / V_P = \gamma = \text{konstan} \qquad (2.11)$$
$$\rightarrow \ln(Z_S) = \ln(Z_P) + \ln(\gamma)$$

Then we assume Gardner equation connects between the density and acoustic Impedance:

$$\rho = aV_P^b$$
$$\rightarrow \ln(\rho) = \frac{b}{1+b}\ln(Z_P) + \frac{\ln(a)}{1+b} \qquad (2.12)$$

Where ρ is density, Vp is the P-wave velocity, *a* and *b* are constant. The two assumptions above imply on the linier relationship between L_p, L_s and L_D. In general, we assume the following equation:

$$\ln(Z_S) = k\ln(Z_P) + k_c + \Delta L_S$$
$$\ln(\rho) = m\ln(Z_P) + m_c + \Delta L_D \qquad (2.13)$$

Where the coefficients k, k_c, m, and m_c will be determined by analyzing the well log data. Figure 2.10 shows the relationship between ln (Z_p) vs ln (Z_s) and ln (Z_p) vs ln (density) of the well log data. The regression coefficient obtained by drawing a straight line on the interesting trend of the data. The retrieved value are K = 1.95, Kc= -2.54, m = 0.25 and mc = - 1.775.

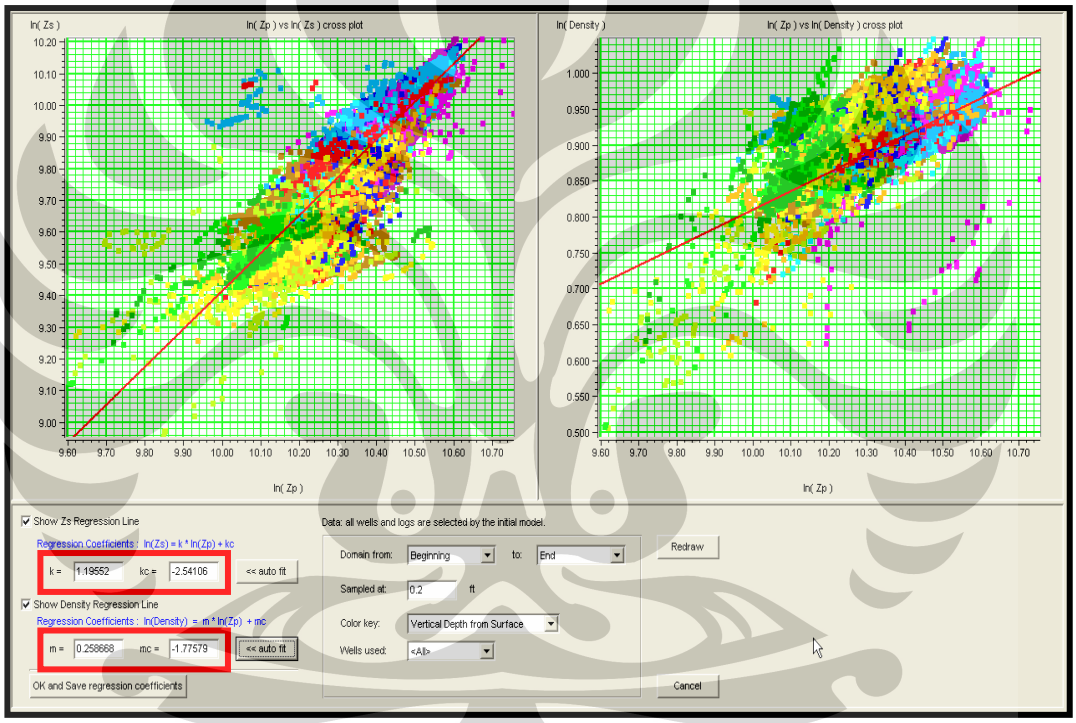

Figure 2.10. A crossplot of ln (Z_p) vs ln (Z_s) and ln (Z_p) vs ln (density) of the well log data, to retrieve K, kc, m, and mc value

Aki-Richards equation becomes:

$$T(\theta) = \tilde{c}_1 W(\theta) D L_P + \tilde{c}_2 W(\theta) D \Delta L_S + c_3 W(\theta) D \Delta L_D \qquad (2.14)$$

where

$$\tilde{c}_1 = (1/2)c_1 + (1/2)kc_2 + mc_3$$
$$\tilde{c}_2 = (1/2)c_2 \qquad (2.15)$$

With the assumption the number of trace is N from various angles, we get:

$$\begin{bmatrix} T(\theta_1) \\ T(\theta_2) \\ \vdots \\ T(\theta_N) \end{bmatrix} = \begin{bmatrix} \tilde{c}_1(\theta_1)W(\theta_1)D & \tilde{c}_2(\theta_1)W(\theta_1)D & c_3(\theta_1)W(\theta_1)D \\ \tilde{c}_1(\theta_2)W(\theta_2)D & \tilde{c}_2(\theta_2)W(\theta_2)D & c_3(\theta_2)W(\theta_2)D \\ \vdots & \vdots & \vdots \\ \tilde{c}_1(\theta_N)W(\theta_N)D & \tilde{c}_2(\theta_N)W(\theta_N)D & c_3(\theta_N)W(\theta_N)D \end{bmatrix} \begin{bmatrix} L_P \\ \Delta L_S \\ \Delta L_D \end{bmatrix} \qquad (2.16)$$

Initial guess is determined with the equation:

$$\begin{bmatrix} L_P & L_S & \Delta L_D \end{bmatrix}^T = \begin{bmatrix} \log(Z_P) & 0 & 0 \end{bmatrix}^T \qquad (2.17)$$

Finally, the value of P-Impedance, S-Impedance and density can be calculated:

$$Z_P = \exp(L_P)$$
$$Z_S = \exp(kL_P + k_c + \Delta L_S) \qquad (2.18)$$
$$\rho = \exp(mL_P + m_c + \Delta L_D)$$

Chapter Three:
DATA AND METHODOLOGY

3.1. INPUT DATA

3.1.1 Well data

The data preparation consisted of identification of the well and 3D seismic data. The well information is sparse within the coverage of the 3D survey, selected based on shear wave log availability. There are 4 (four) wells are used in this study which has shear wave information for identifying rock physics and elastic properties of Menggala formation, they are: DEFI-09, DEFI-10, DEFI-11, and DEFI-15. As shear information can be crucial for discriminating lithologic and pore fluid ambiguities, a calibration well outside the study area may be performed in this method. The well data had been subjected to an extensive petrophysical analysis prior to this study. Additional data, such as checkshot survey and production test result are obtained from DEFI-01 exploration well since the key wells mentioned above do not have this data. Checkshot survey is required for time depth conversion and well seismic tie, while production test data is required to be input as reservoir properties in fluid substitution method. Well location on the Lower Menggala Depth Structure Map is showed on figure 3.1.

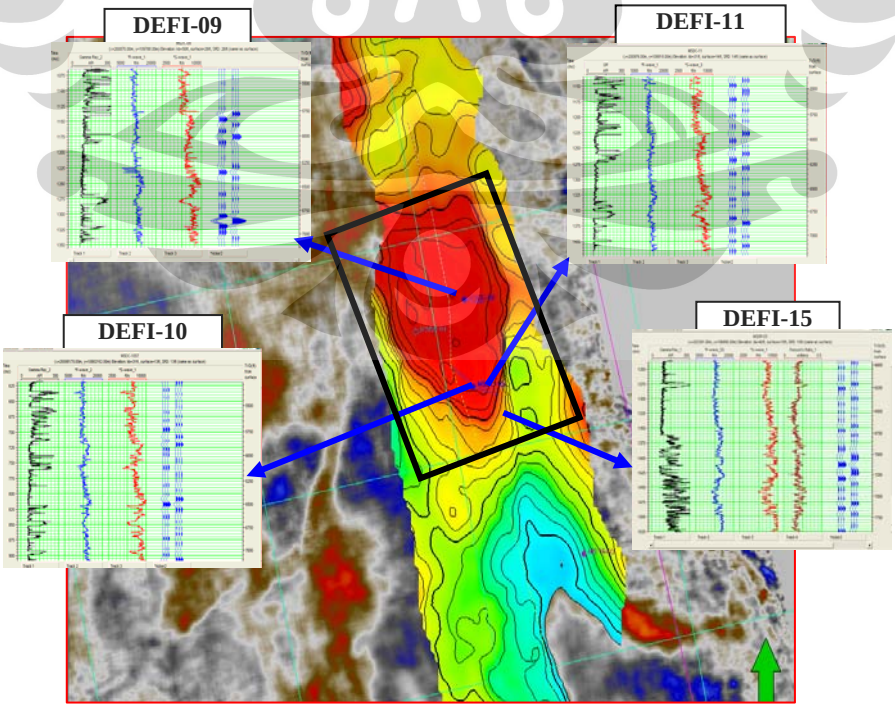

Figure 3.1. Key well location on Lower Menggala Depth Structure Map

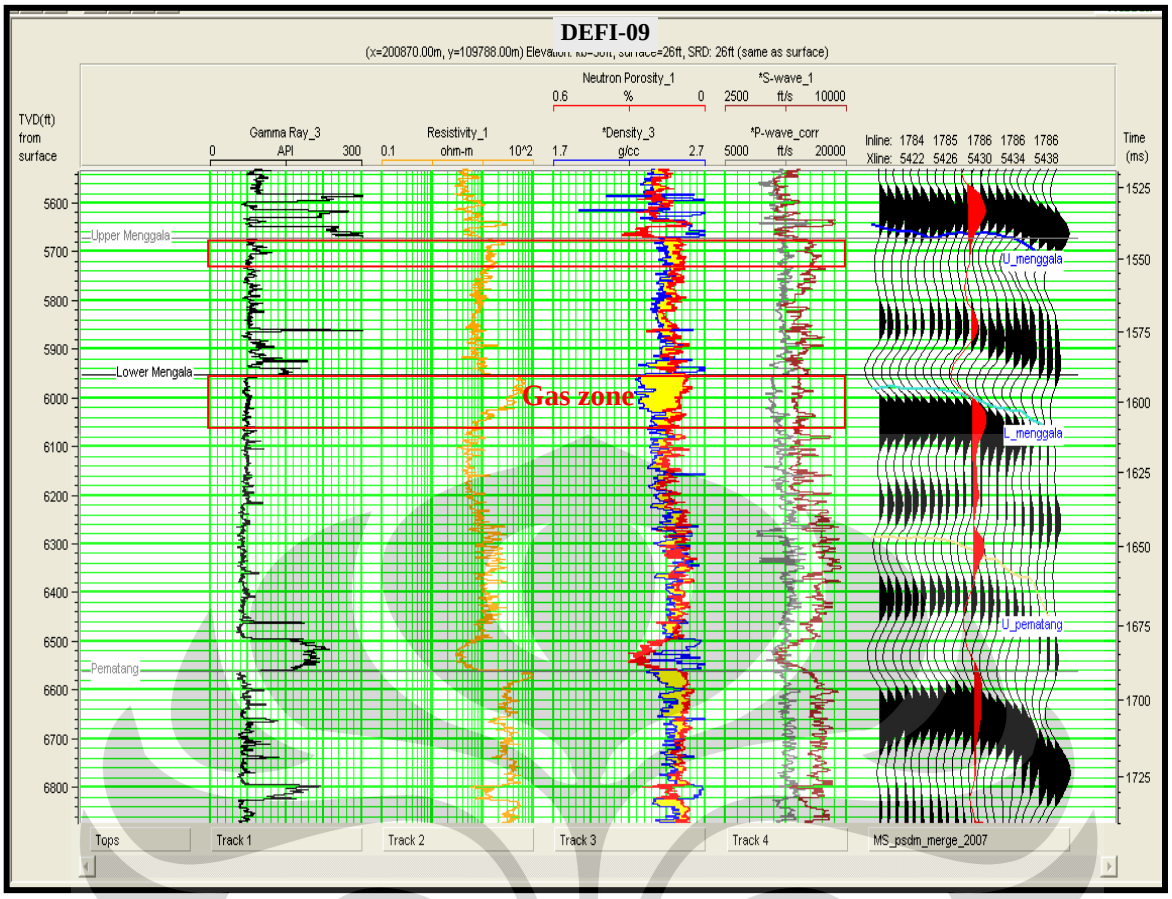

Figure 3.2 DEFI-09 well log display, interesting zone indicated by red box on top of Upper and Lower Menggala formation

3.1.2 Seismic data

The seismic data used in this study is a angle gather volume from a 3D survey covering DEFI field (figure 3.3). The area is limited by inline 1730 – 1900 and crossline 5350-5480. The seismic was processed for preserved amplitude to optimize inversion process. All processes are done before this research by following the standard seismic processing methods, except some of the amplitude gain method to maintain the preserved amplitude as mentioned above. Angle gather data is then partial stacked to eliminate the influence of noise recorded by the seismic. Partial stacking is based on the amplitude changes versus the angle of incident wave. Therefore the picking analysis is required at the level of interval studied as showed on figure 3.4, by plotting the amplitude gradient versus angle and divided the trace qualitatively. The seismic traces in the range of angle 0-12^0, are stacked as near angle volume based on low contrast gradient on amplitude versus angle. A higher gradient changes is observed in the range of angle 12-27^0 and it is stacked as mid angle seismic

volume. The rest trace seismic in the range of angle 27-42^0 showing high contrast gradient on amplitude versus angle and it is stacked as far angle seismic volume. The stacking result is showed on figure 3.5. Thus, the partial stacking is expected to reduce the influence of noise in the recorded seismic data so that minimize the potential misinterpretation of seismic inversion. A larger 3D post stack seismic data (covering surrounding field of DEFI structure) is used to perform regional horizon interpretation and support geological model. The interval of interest ranges in this seismic process is from 1500 – 1800 ms (TWT) covering Upper and Lower Menggala reservoir, with seismic resolution is calculated to be 25 ms vertically.

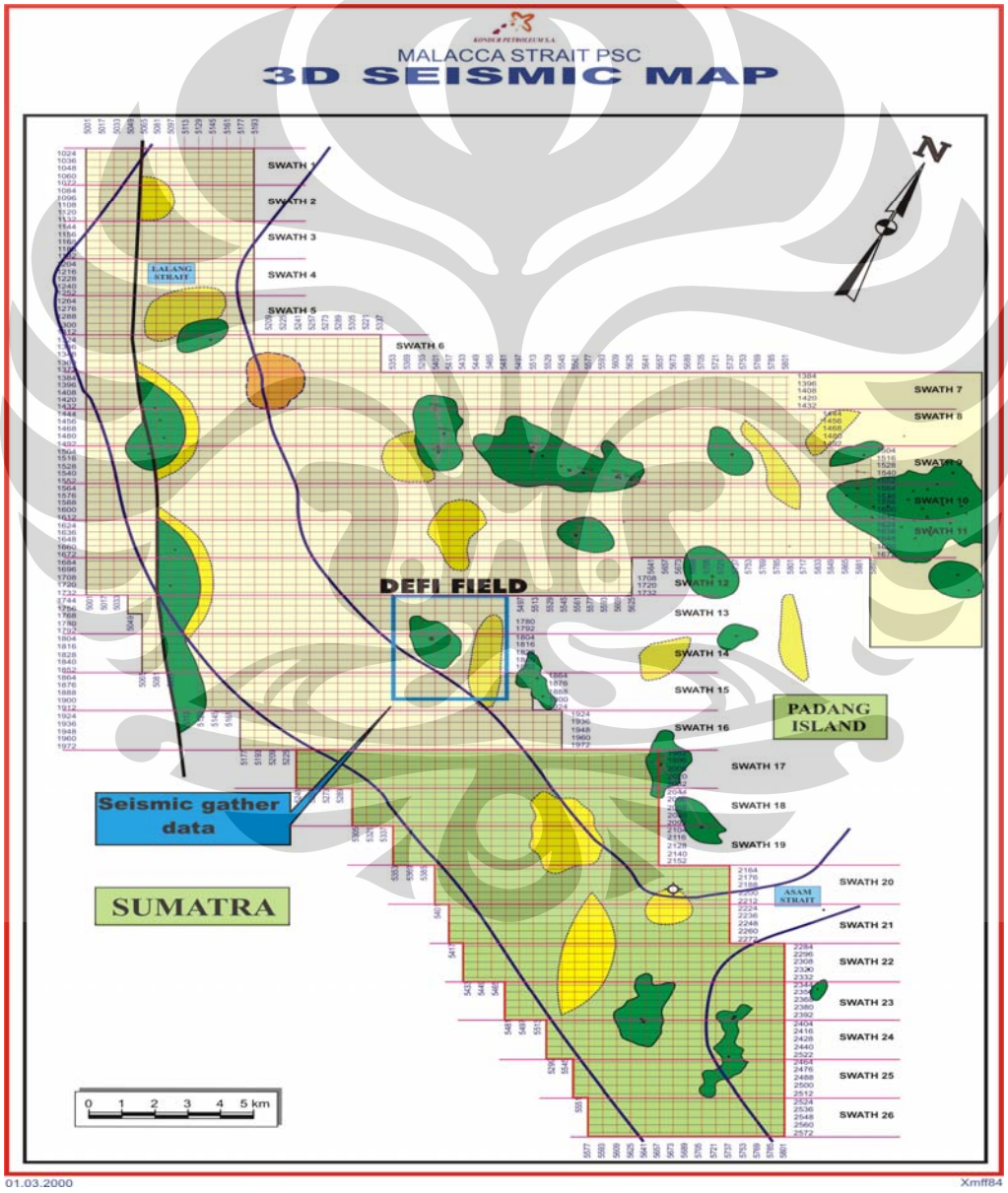

Figure 3.3 3D Seismic Base Map in The Malacca Strait Block, data to be processed for simultaneous inversion is limited by inline 1730 – 1900 and crossline 5350-5480, covering DEFI field

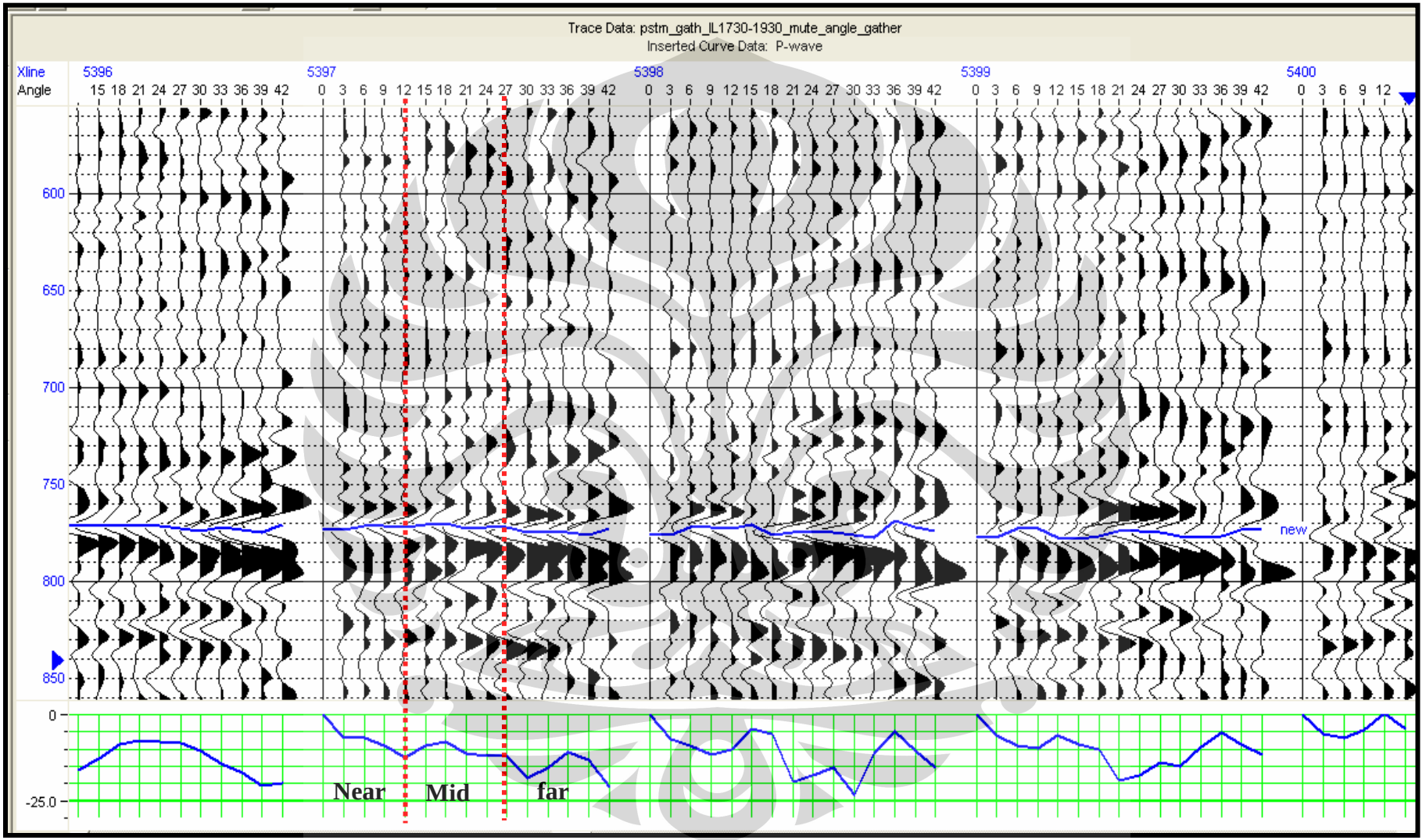

Figure 3.4. Seismic gather data prior to partially stacking based on amplitude response against offset. The horizon is top of Lower Menggala

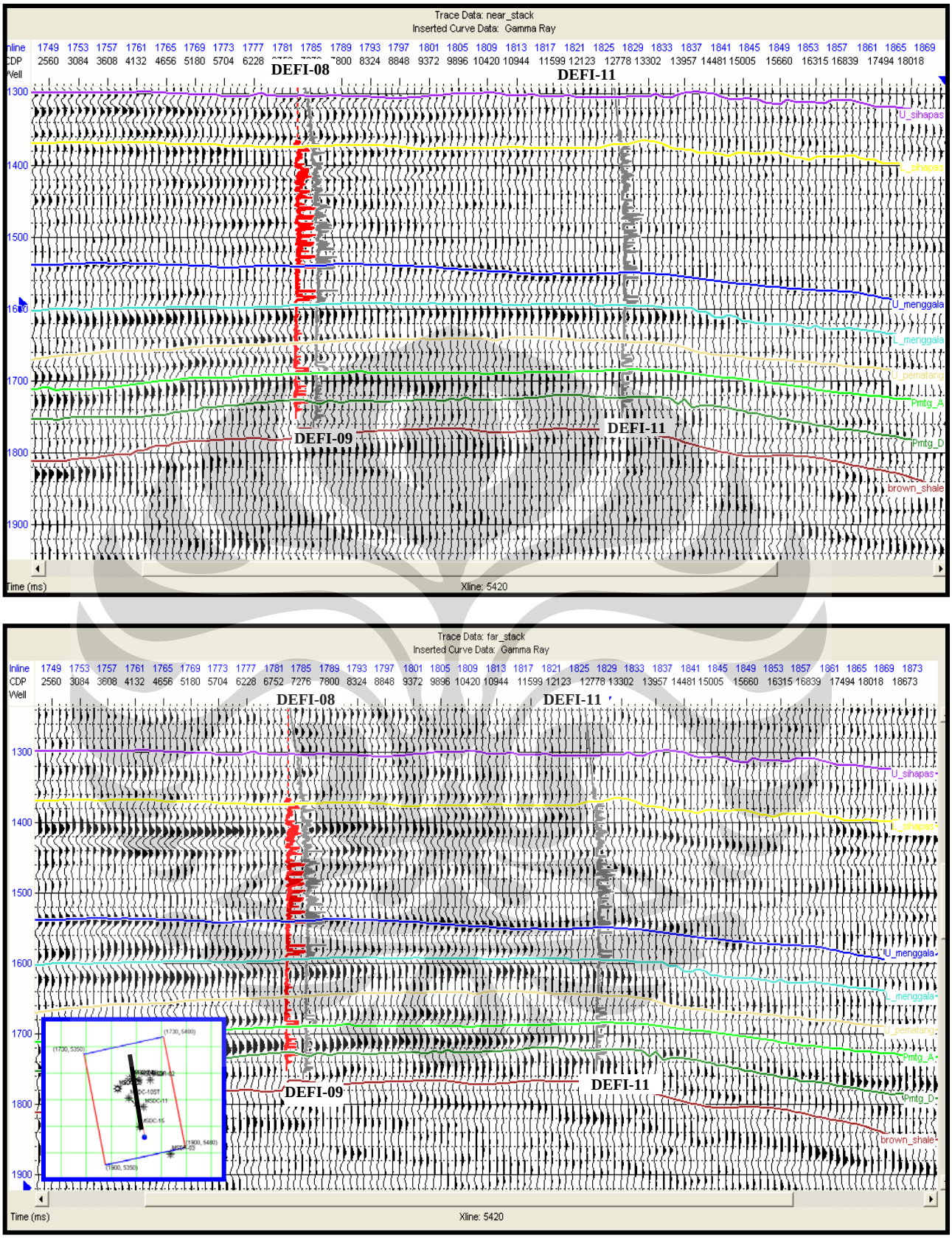

Figure 3.5. The partial stacking result based on amplitude analysis versus angle of incident. The near angle seismic volume **(top)** represents trace seismic recorded in the range of angle 0-12^0 and Far angle seismic volume **(bottom)** is represents trace seismic in the range of angle 27-42^0 (The mid angle seismic volume is not displayed in this figure). The section is N-S line (Xline) across DEFI wells

3.2. METHODOLOGY

The study methodology is divided in 2 (two) phase based on data to be handle and processed, they are: well based rock physics analysis as phase 1 and seismic simultaneous inversion as phase 2. The workflow is summarized in figure 3.6. These steps will be done if assuming that quality control and corrections of well logs and seismic data has been performed. The workflow is described below:

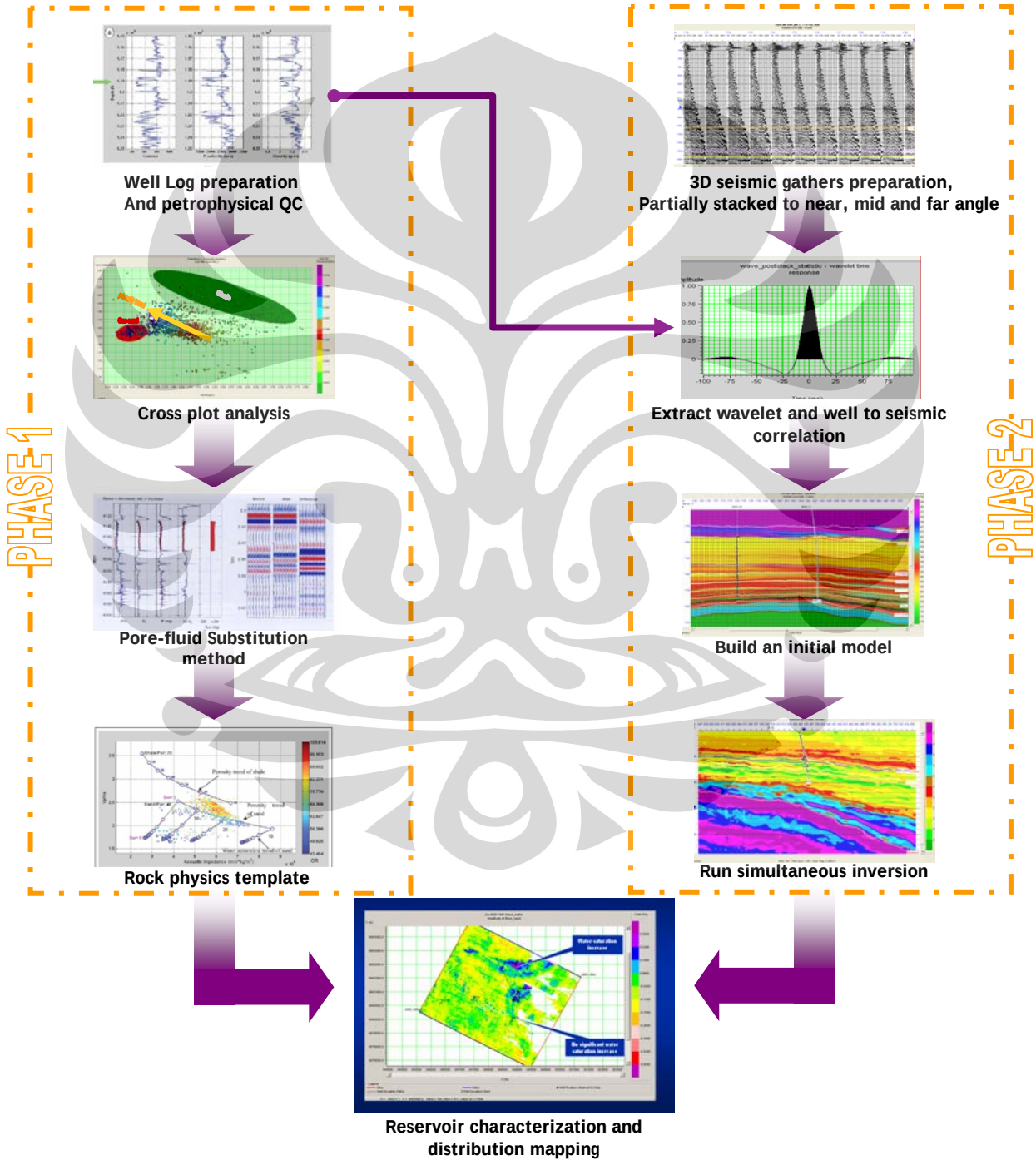

Figure 3.6. The workflow, from Rock physics to reservoir characterization

3.2.1 Well log based- Rock Physics Analysis (Phase I)

1. Cross plot Analysis

   To test sensitivity of seismic parameter with the petrophysical properties, cross plots of different well log data is performed prior to generate rock physics model. Cross plot analysis is performed in each key well data with same parameter for building Rock Physics Template (RPT) at the end of this phase. DEFI-09 petrophysical data is one of good example which sensitive to seismic parameter (as shown in figure 2.1, chapter 1). Three basic seismic parameter (Vp, Vs and density) are showing ability to separate gas sand, brine sand and shale. These basic parameters are also transformed in a particular parameter to see more trend of petrophysical properties, including P-impedance, and S-impedance The lithologic and fluid content interpretation is based on a suite different log data (gamma ray, resistivity, density and neutron logs). Color coded scatter plots indicating a third dimension of gamma ray, saturation, clay content, or other petrophysical logs. The third dimension helps to identify the reasons for trends observed in the cross plots and will be apply for rock physics model at the end of this phase.

2. Pore-fluid substitution

   In order to generate Rock physics model, a fluid substitution to find out what if fluids change? What happens to seismic parameters behavior? Figure 3.7 shows DEFI-09 well logs penetrating the Menggala formation. Along with it is the corresponding seismic synthetic as convolution result of P-wave and density with wavelet extracted statistically from seismic data. The initial logs shows an average water saturation of about 90% in the most upper and lower Menggala sand, except a gas saturated zone observed at the top of formation. We apply a Biot Gassman fluid substitution decreasing the water saturation to 30% with the following reservoir properties obtained from DEFI-01 exploration well production test data:

   Formation pressure : 2509 Psi
   Gas gravity : 0.79
   Temperature : 299^0F
   GOR : 51685 cft/bbls
   Water salinity : 6700 ppm

The program used for fluid replacement method then calculated the Bulk modulus of water and gas to be input in Biot-Gassman equation as follow:

K_{water} : 2.1551 GPa

K_{gas} : 0.0341 GPa

ρ_{water} : 0.9345 g/cc

ρ_{gas} : 0.1227 g/cc

The predicted result is shown on the same track as initial logs with different color and log name for the fluid substitution result (a FRM abbreviation and grey color is logs after fluid substituted, while the blue one is the initial logs). On the water zone, we see that replacing water with gas decreases slightly density and P-wave velocity in the Menggala sand, therefore the impedance decreases by about 3%. The less decreases bring forth to porosity substitution to predict seismic parameter changes related to reservoir properties

Since fluid substitution resulting less change in seismic parameter, we perform porosity substitution to capture what happens if porosity changes? Figure 3.8 is same well penetrating Menggala formation in the DEFI field. Bulk modulus and density of fluid to be inputted is same with the fluid substitution method, as same as parameter of mineral as follow:

$K_{mineral}$: 20.9891 GPa

$\mu_{mineral}$: 6.98533 GPa

$\rho_{mineral}$: 2.58069 g/cc

The bulk modulus, shear modulus and density of mineral are calculated from petrophysical logs of mineral volume (quartz and clay). By applying Biot-Gassman, now we predict porosity reduction to 5 % from an average 15 % of initial logs (a PRM abbreviation and red color is logs after fluid substituted, while the blue one is the initial logs).We see that decreasing porosity cause large increases density, P-wave velocity and S-wave velocity. This change raises strong presumptions that porosity will be confident to be detected in seismic scale

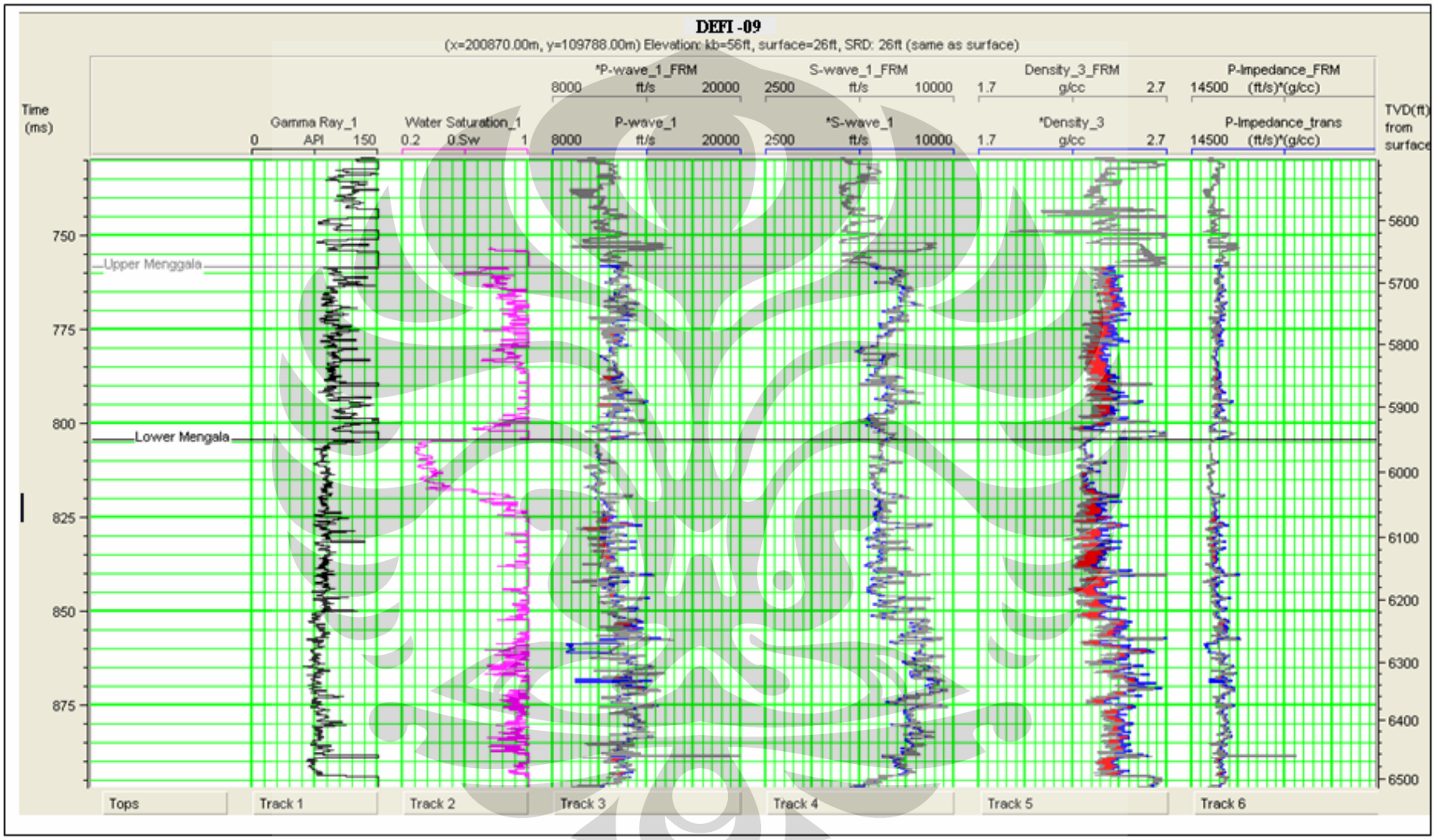

Figure 3.7. Well logs display after decreasing water saturation from 90% to 30 %, decreases slightly density and P-wave (red shade)

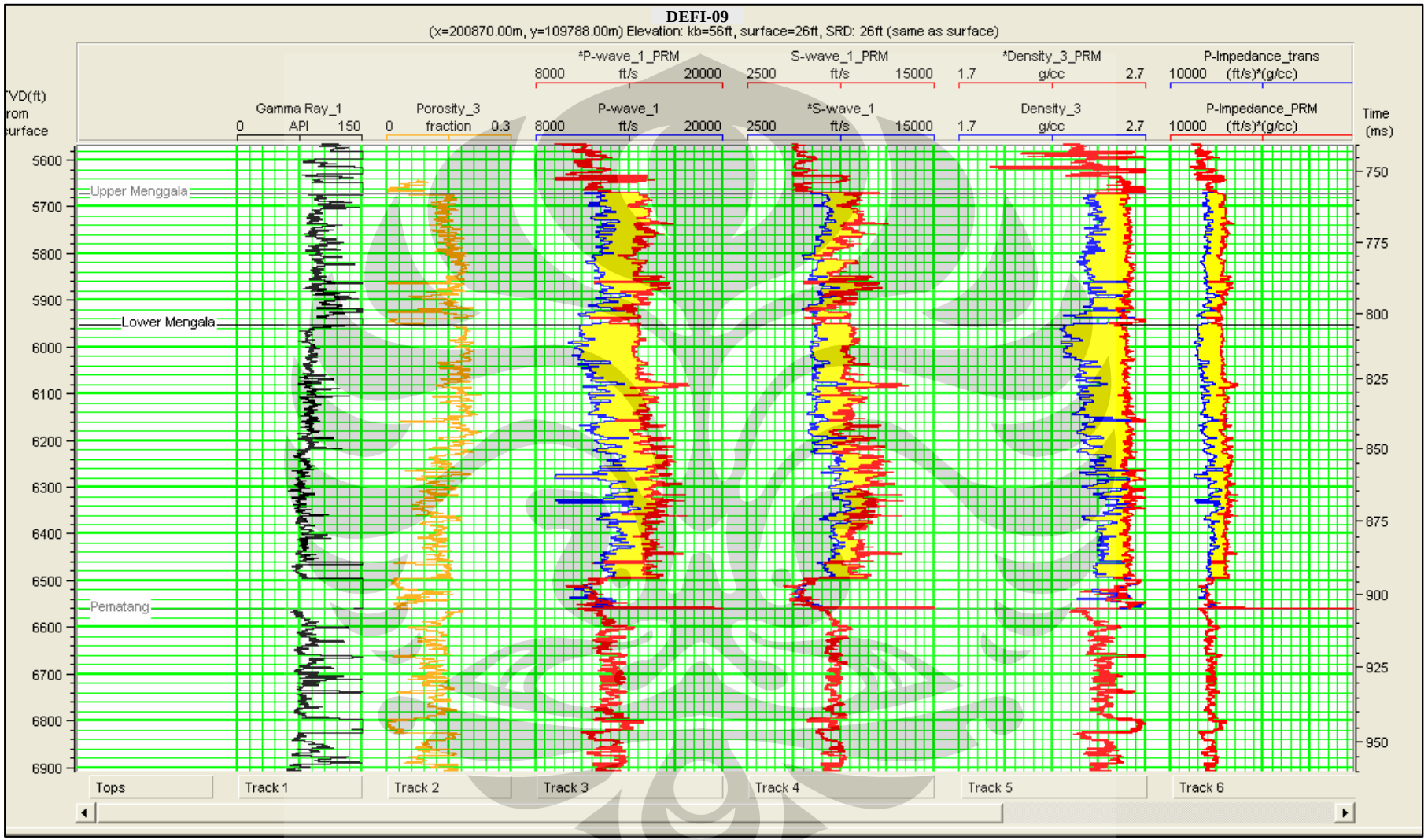

Figure 3.8. Well logs display after porosity reduction from 18% average to 5 %, increases largely density, S-wave and P-wave (yellow shade)

3. Rock Physic Template (RPT)

Rock physic modeling will be the last step in the phase 1 before entering into the simultaneous inversion workflow. After sensitivity test and pore fluid substitution are performed on all key well data, then all parameter are plot in the same scale and same template for defining the rock physic model in the DEFI structure. This template, which known as the Rock Physics Template (RPT), will be used as a guide in mapping pore fluid distribution on the seismic scale. Reservoir characters that will be mapped, represented by color code on the third dimensions (Vsh, porosity and water saturation). Figure 3.9 shows how the P- impedance and S-impedance able to separate the sand and shale interval, porosity trend, and gas zone for all wells the analyzed in DEFI field. For characterization with the Vp/Vs ratio versus P-Impedance parameter, data from DEFI-09, DEFI-10, DEFI-11 and DEFI-15 well show same trend (figure 3.7). The discussion of the RPT analysis is described in chapter 4

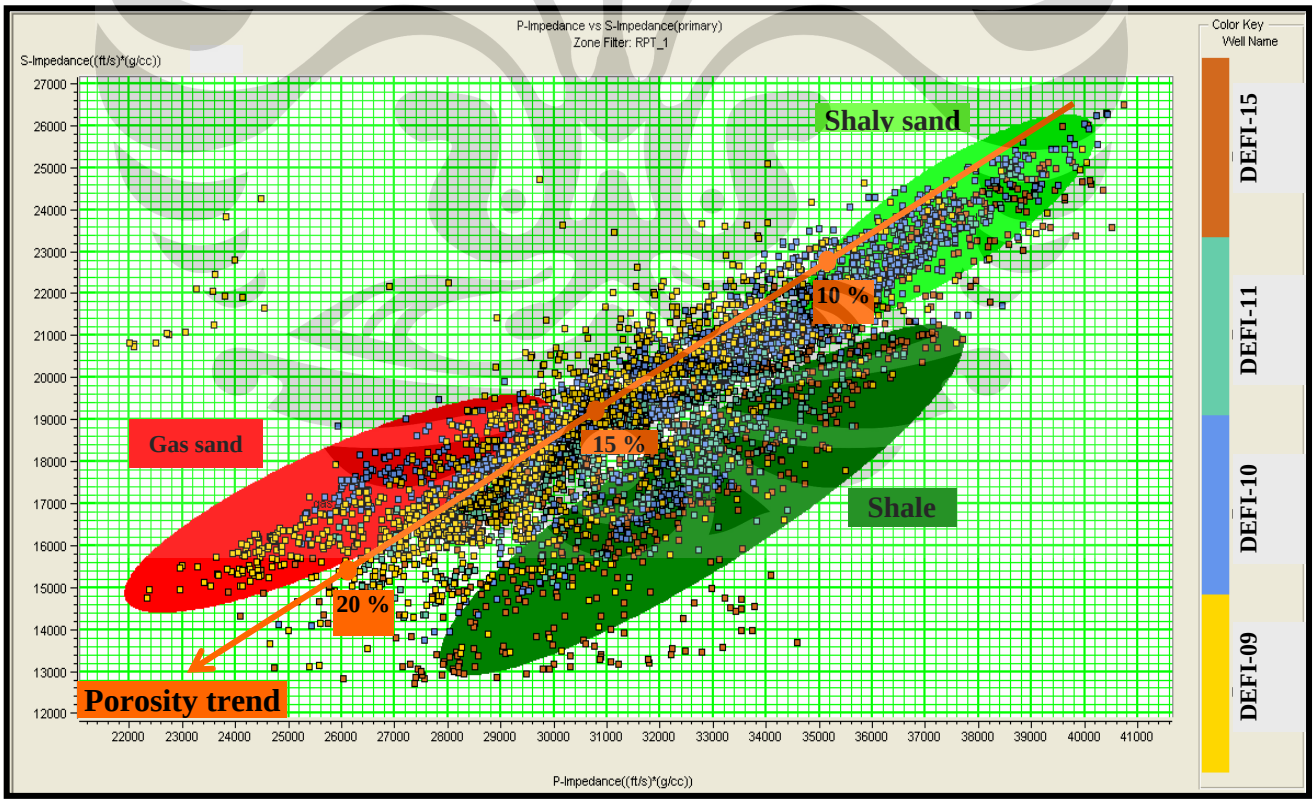

Figure 3.9. Rock Physics Template (RPT) for Menggala formation at DEFI field. Data are compiled from several crossplot using different petrophysical color codes (Vsh, porosity, and water saturation)

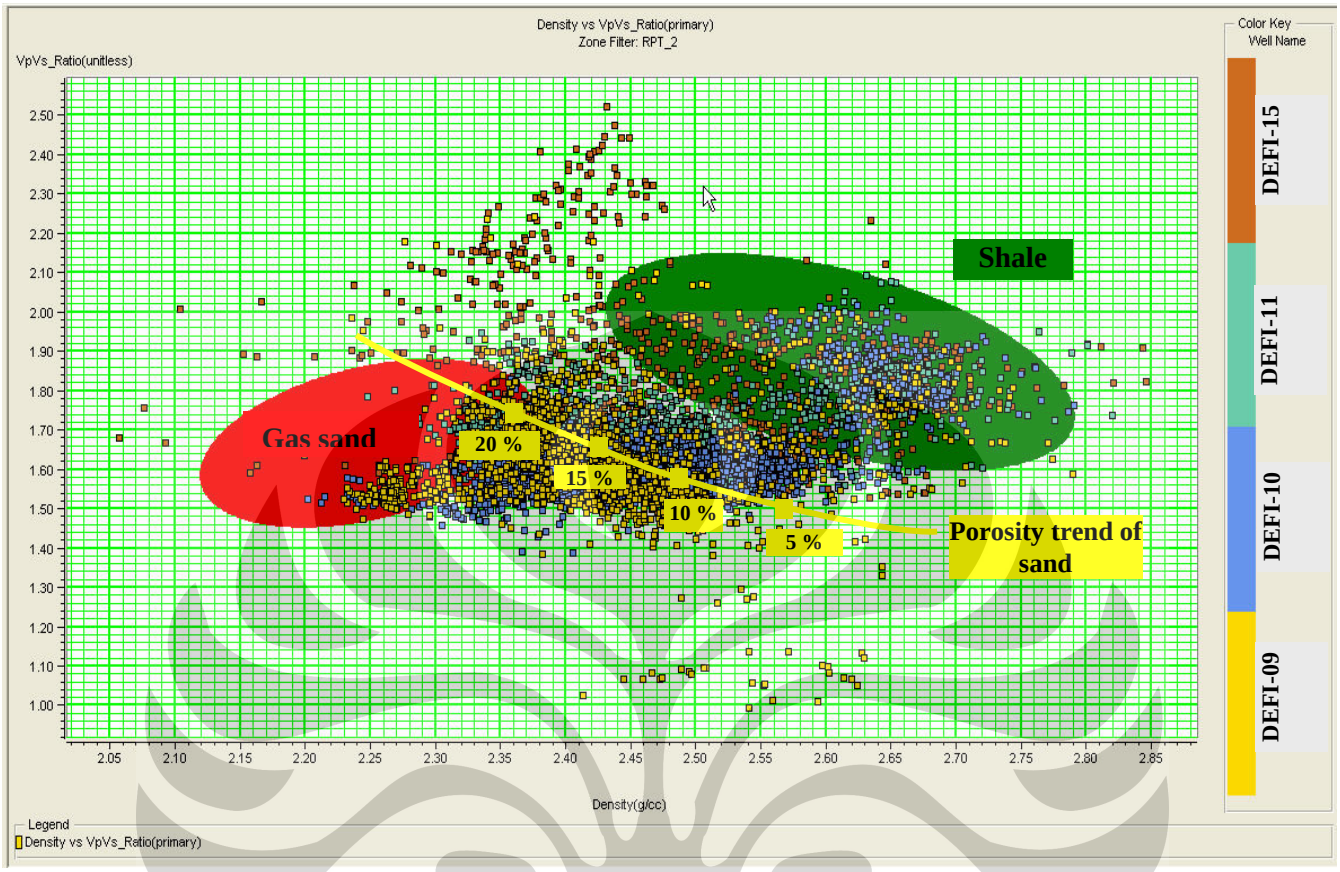

Figure 3.10 RPT with Vp/Vs ratio versus AI showing same trend as functions of porosity and gas effects on Menggala formation

3.2.2 Simultaneous Seismic Inversion (Phase II)

As described previously, simultaneous inversion method is using partial data stack (near, mid and far stack) to get information of P-impedance, S-impedance, and density simultaneously as defined by well log based-rock physics analysis. Partial stacking process has been explained previously in the seismic data preparation on section 3.1.2. Seismic data to be input are consisting of a near angle stack ($0\text{-}12^0$), mid angle stack ($12\text{-}27^0$) and far angle stack ($27\text{-}42^0$) from the seismic gather, and it is loaded by regional horizon which have been picked previously on another project. Since all the horizons are picked on post stack seismic, so the values are drawn flat across each other. Once all seismic and horizons have been loaded into database, the workflow then continued to correlate seismic to well data using wavelet extracted from seismic and constraint by checkshot and well log data.

1. Wavelet Extraction

The wavelet Extraction procedure uses the seismic traces alone to extract the wavelet statistically. It extracts the wavelet amplitude spectrum by analyzing the autocorrelation of a set of traces over a selected time window, from Upper Menggala horizon at 1500's ms to Lower Menggala horizon at 1800's ms. In this procedure, the phase of the wavelet cannot be determined from the data itself, zero phase is the default and is commonly used for wavelets for log correlation. The amplitude spectrum is calculated using the autocorrelation of the seismic trace. Wavelet extraction process is done for the entire data stack angle (near, mid and far offset) to get angle dependent wavelet for simultaneous inversion process. The dominant frequency of seismic data is 20 Hz where wavelet length is set to 200 ms. To generate synthetic seismogram from well data, the extracted wavelet was convoluted with Reflection coefficients which is obtained from contract impedance. This synthetic seismic is used for well-seismic tie at the level of interest. Figure 3.11 shows an example seismic tying to DEFI-01 well by using the wavelet extracted statistically from near and far angle stacked seismic. The correlation result comes with 70% correlation coefficient both on near and far seismic. This is a good indication that seismic we analyzed is tied to well observed, as also indicated by good correlation coefficient (> 0.7) on other wells at DEFI field.

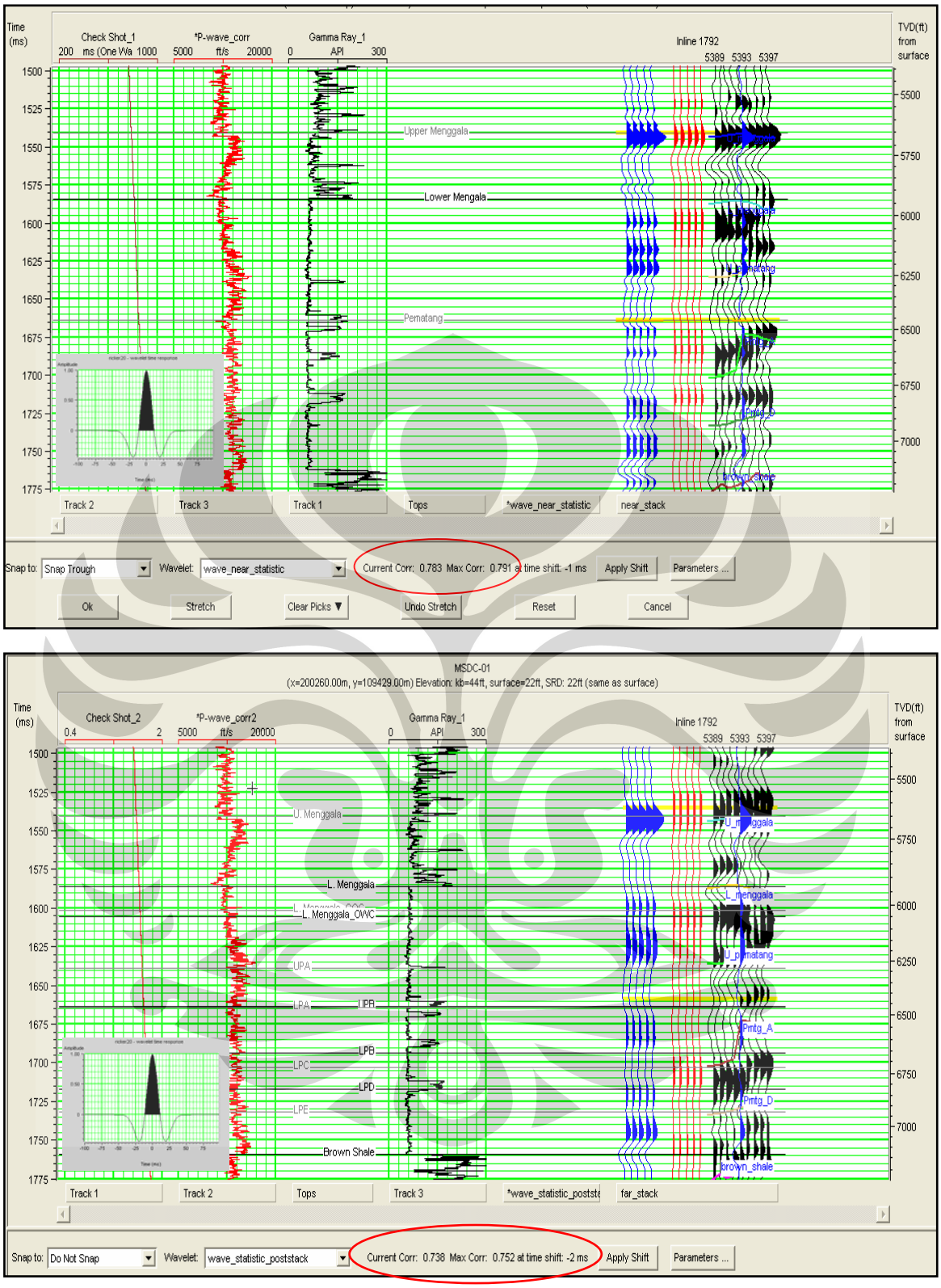

Figure 3.11 DEFI-01 well to seismic near-far stack correlation with correlation coefficients of 0.7 for near angle stack (top), and far angle stack (bottom). The wavelet is extracted from seismic statistically.

2. Building Initial Model

Initial model building is determined by the results of horizon picking/interpretation and well log data which is represents the rock physics character by P-impedance, S-impedance and density log. Model is a representation of the data well as vertical control, while the laterals control using seismic data that the horizon has been interpreted. In building this initial model, Log data used are from DEFI-09, DEFI-10, DEFI-11 and DEFI-15 as a vertical control, while horizontal control using the horizon of Upper Menggala, Lower Menggala, and Upper Pematang. Log data used in this model is has been corrected from well-seismic correlation, means the time depth curve has been corrected as well so that the scale of the log data in accordance with the time in the seismic data. Section below shows the initial model of P-Impedance on the trajectory taken through DEFI-09 well (figure 3.12). There are also initial model of S-impedance and initial model of density resulted in this method but they do not displayed in this section.

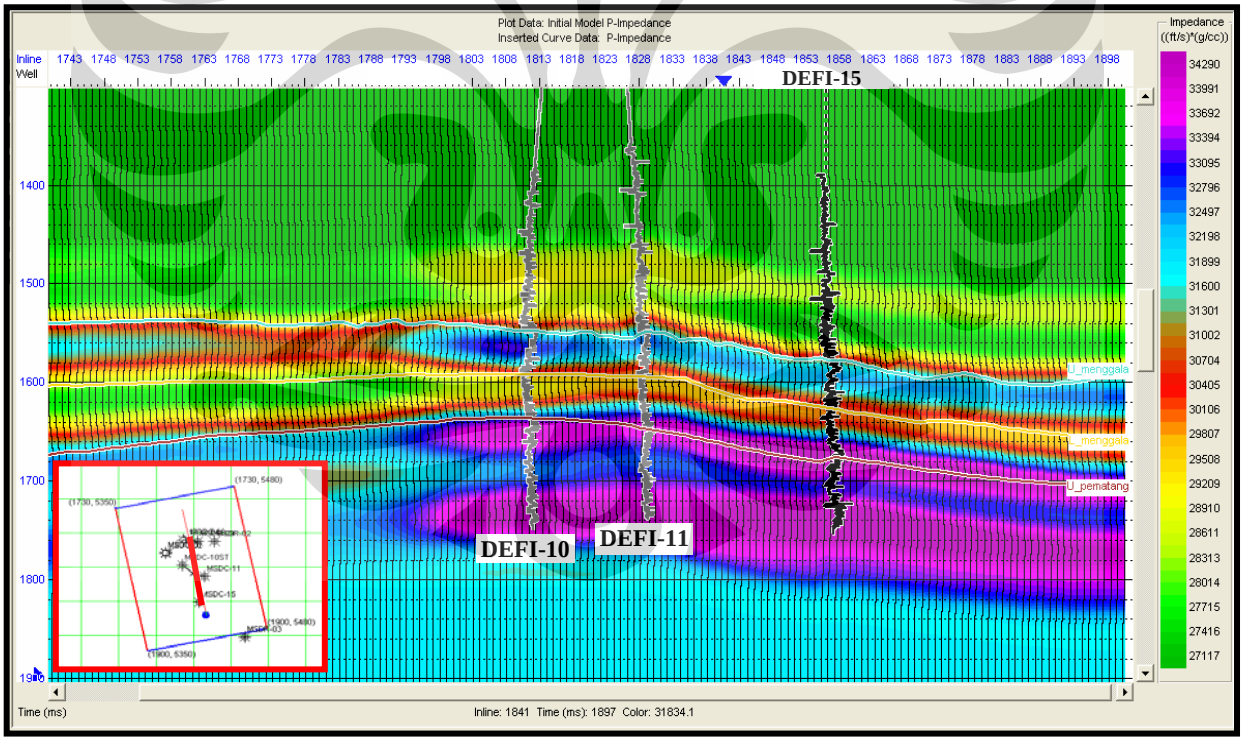

Figure 3.12 Initial model of P-impedance through N-S line of DEFI field. P-impedance curves from well data are inserted to indicate that the model is built based on P-impedance log

3. Simultaneous Inversion Process

Simultaneous inversion is the final process of partial angle stack (near, mid and far) which are inverted together with wavelet estimation of each seismic angle stack to obtain the information P-impedance, S-impedance, Density and Vp/Vs ratio. From Aki-Richards equation which was discussed in chapter 2 note that reflectivity is a function of Vp, Vs, density and angle, then the information from the data input is generated a relationship between the four parameters. As the initial model is the reference, we then run the simultaneous inversion. Algorithm used in the inversion program is a least square based-conjugate gradient. Algorithms attempt to answer this problem of non-linier inversion. In general, the algorithm used in the simultaneous inversion of the program is as follows:

- Input data: n trace seismic data from various incident angle, n wavelet (one wavelet for each incident angle), the initials Zp, Zs and density.
- Calculate the constant k, kc, m, and mc from regression analysis of well trend data (figure 3.13)
- Determine the initial guess using the equation 2.17
- Solve the equation system with the conjugate gradient method.
- Calculate the value of Zp, Zs and the density using the 2.18 equation

Results from a simultaneous inversion process are P-Impedance, S-impedance and density model. Figure 3.14 shows the simultaneous inversion results for P-Impedance, S-impedance and density. The inversion analysis window performs an inversion on selected well locations, which means we can analyze a range of inversion parameters to well log data (figure 3.15). By comparing well data in the model and inverted section, in general we can justify that inversion results have a good correlation with the well data.

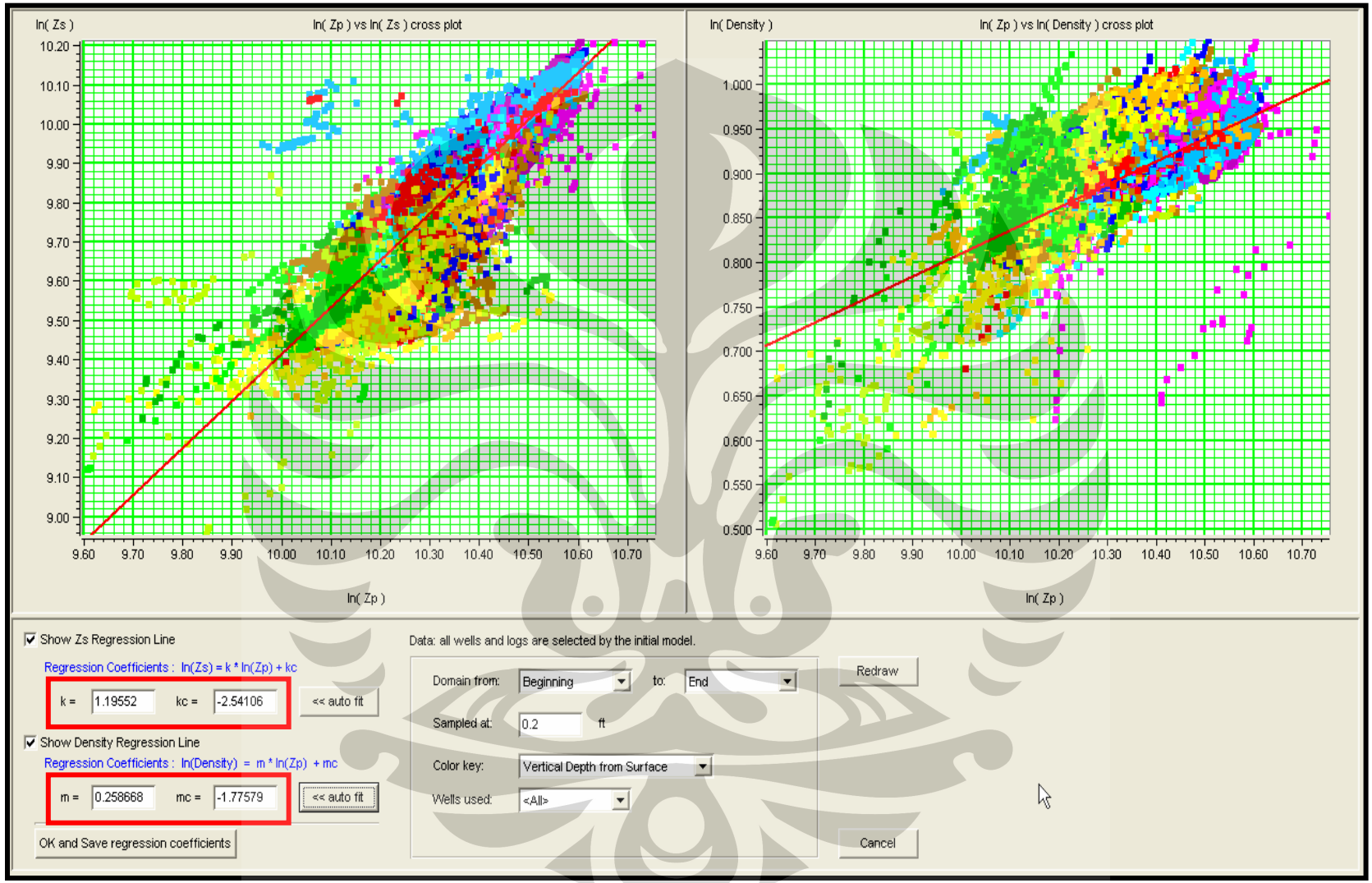

Figure 3.13 Cross plots of ln(r) vs ln(ZP) and ln(ZS) vs ln(ZP) from DEFI wells. In both cases, a best straight line fit has been added to obtain k, kc, m, and mc value

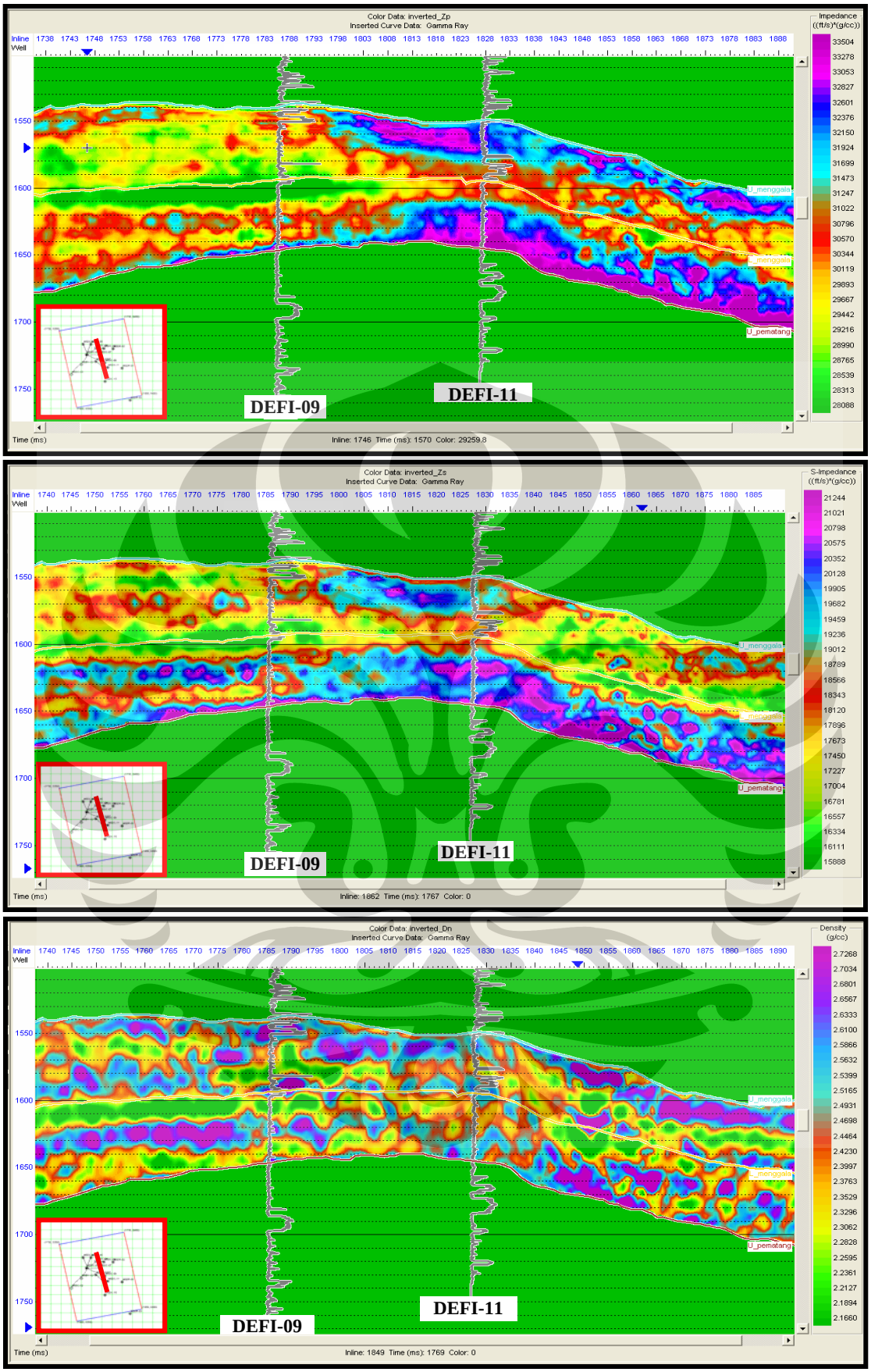

Figure 3.14 Inversion result from 3 seismic angle stack (near, mid, far) in the level of Upper and Lower Menggala, generates 3 volume simultaneously: inverted P-impedance (top), inverted S-impedance (middle) and Inverted density (bottom) through N-S line of DEFI field

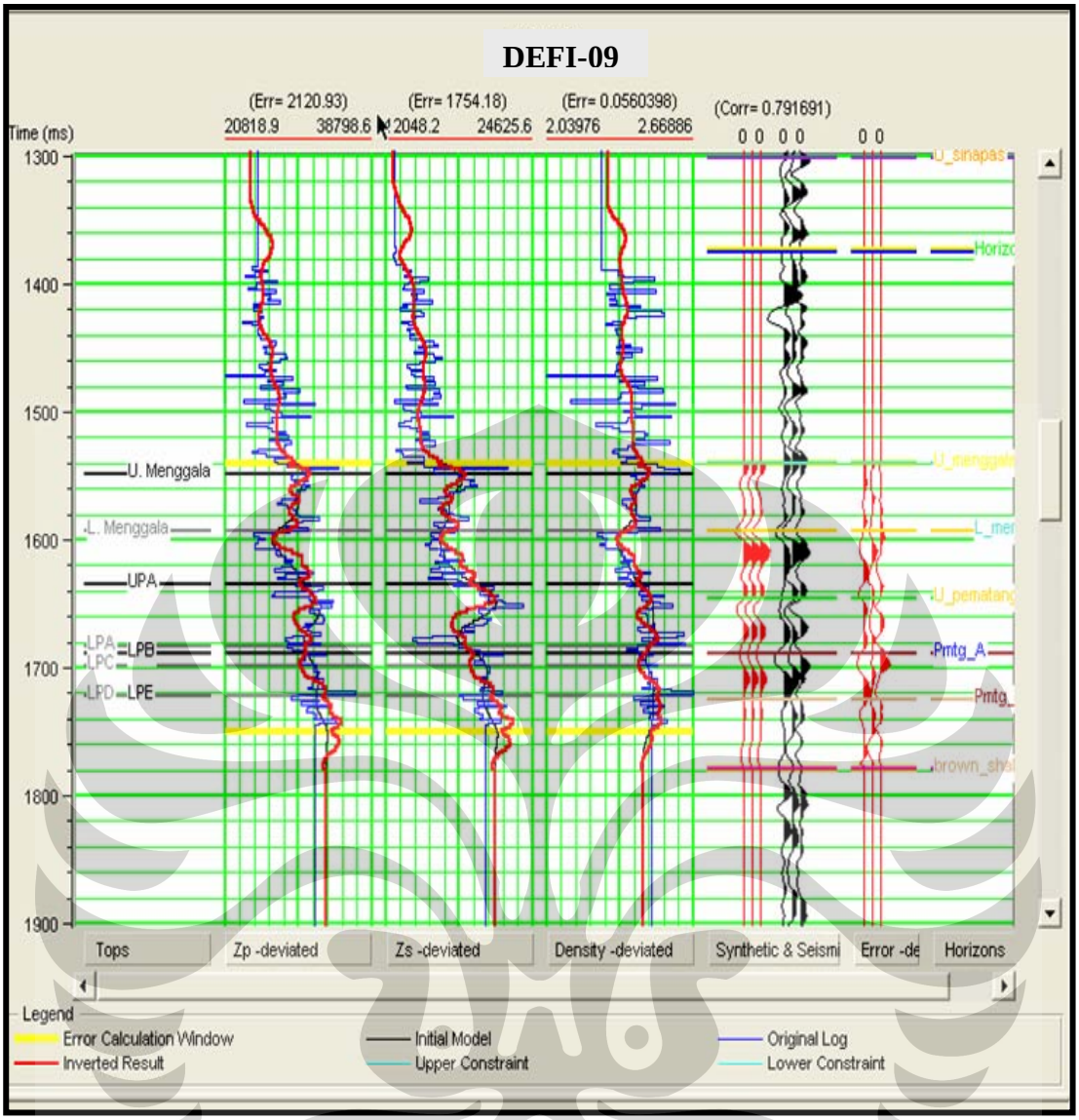

Figure 3.15 The inversion analysis window on selected DEFI-09 well location comparing log curves, initial model and inversion result.

Chapter Four:
ANALYSIS AND INTERPRETATION

4.1. Rock Physics Interpretation of well log data

As exposed in chapter 3 section 3.2.1, a Rock Physics Template (RPT) has been generated from well log data superimposed to P-impedance versus S-impedance and Vp/vs ratio versus density with petrohyisical value as color coded. The petrophysical interpretation is based on suite of different log (GR, Resistivity, density and Neutron) as well as reservoir information from core and well DST (see chapter 2, section 2.1 and 2.2). We have identified certain populations in the data and marked these with trend lines and colored zones. The line and boundary of zone are selected by qualitative judgement based on petrophysical value. Figure 4.1 show how the shale zone is generated from Vsh separation by P-impedance vs S-impedance crossplot. We cut off Vsh at 60% as shale line where lithology has Vsh below 60% is interpreted as sandstone. All populations above 60% of Vsh is plotted to shale zone.

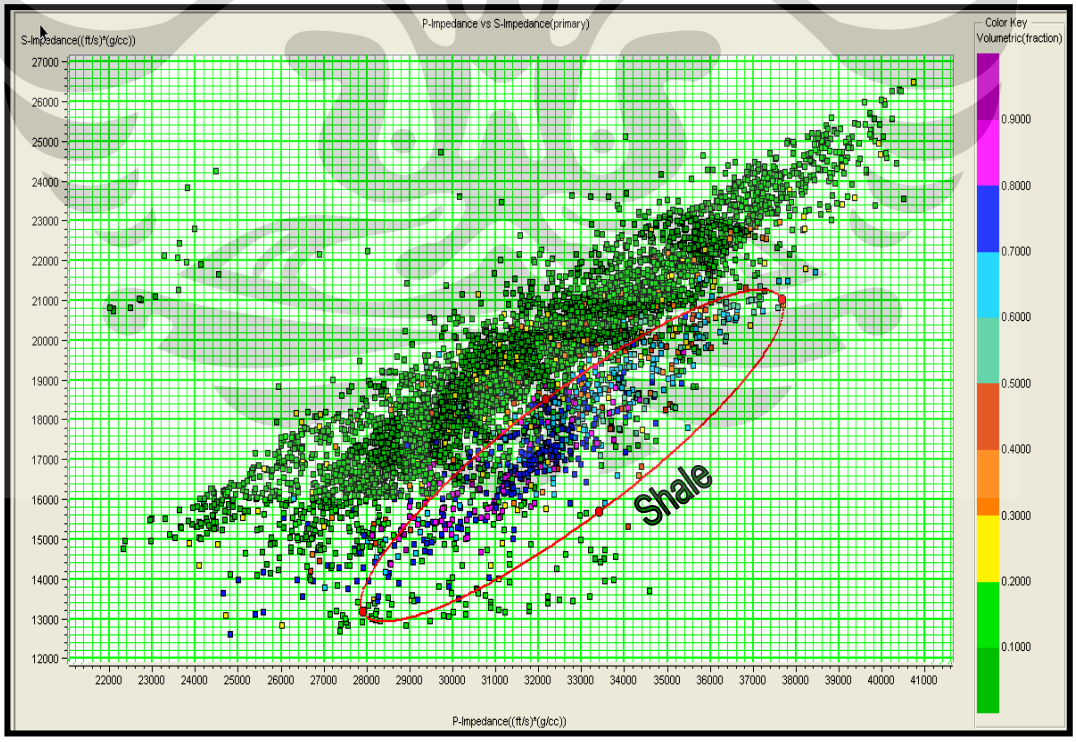

Figure 4.1 P-impedance vs S-impedance color coded by Volume of Shale (Vsh). The shale polygon is defined based on Vsh value above 60 %

The shale clustered is distributed varies from high impedance to low impedance. The trend of shale zone is affected by the trend of porosity and it causes decreasing velocity. This fact is supported by an empirical study by Han (1986) demonstrated the relationship of porosity and clay content with its effect to acoustic properties of sandstone and consolidated sediments. Han plotted Vp and Vs value from seismic versus porosity for a large set of laboratory ultrasonic data for water saturated sandstones. In his plots, the data showed the usual general trend of decreasing velocity with increasing porosity. There is a great deal of scatter around the trend, which we know from Han's work is well correlated with the clay content. Han described this velocity-porosity-clay behavior with the empirical relations:

$$V_p = 5.59 - 6.93\phi - 2.13C$$

$$V_s = 3.52 - 4.91\phi - 1.89C \qquad (4.1)$$

Where the velocities are in the km/s, ϕ is the porosity and C is the clay volume. As with any empirical relations, when using equations 4.1 is important to consider the coupled effects of porosity and clay. If two rocks have the same porosity but different amounts of clay, then chances are good that high clay rock has lower velocity. But if porosity decreases as clay volume increases, then the high clay rock might have a higher velocity (Avseth et al, 2005).

In term of velocity-shale content relationship, we observed a slightly general trend of increasing Vsh with increasing Vp/Vs ratio as diplayed on figure 4.2. This figure is crossplot of Vp/vs versus density and color coded by Vsh. The shale populations (> 60% Vsh) are clustered on Vp/Vs value above 1.7. Castagna *et al* (1993 vide Avseth et al, 2005) suggest that if the lithology is well known, then one might fine-tune these relations to slightly higher Vp/Vs for high shale content and lower Vp/Vs in cleaner sands. When the lithology is not well constrained, then the Han and Castagna et al lines give a reasonable average. In this study, the lithology is well known so that the Vp/Vs value is usefull for identifiying shale distributions

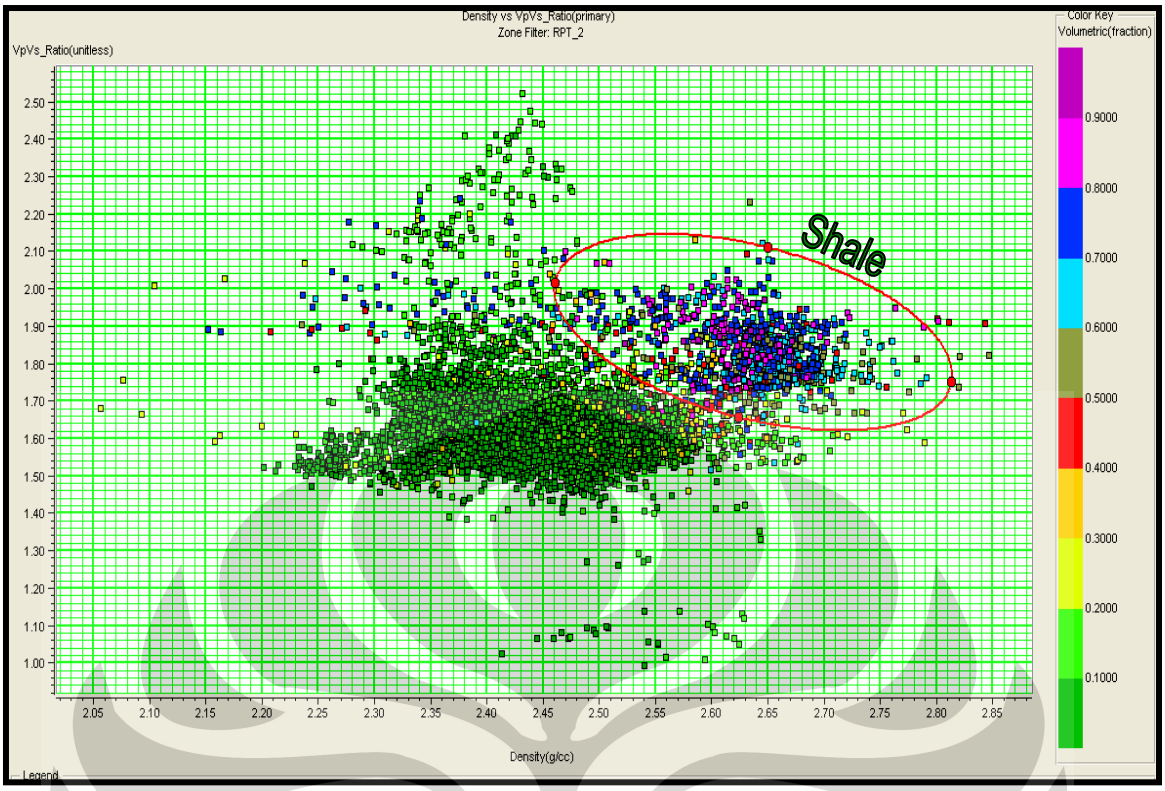

Figure 4.2 Vsh clustered on Density vs Vp/Vs crossplot. Shale populated above 1.7 of Vp/Vs ratio

Rock physis model that relate velocity and impedaance to porosity form a critical part of seismic analysis of porosity and lithofacies. Figure 4.3 show the crossplot of P-impedance vs S-impedance and color coded by porosity from petrophysical analysis. The porosity value used in this analsys is porosity effective that allows fluid content influnence to rock physics parameter. We see here an usual general trend of data that porosity tends to decrease impedance. As discussed in Fluid substitution analysis method (Chapter 3 section 3.2.1), this linear trend could be explained by Gassman (1951) formula that Velocity is affected by bulk modulus and density where porosity and rock matriks are included in both parameters. By this trend, on Rock Physics Template (RPT) we clustered the sand into 2 zones based on porosity property and its impedance. The shaly sand zone is qualitatively judged by low porosity (>10%) where it is populated on high impedance. Cluster on low impedance zone is interpreted as the prospective porous sand with potentially contains water or hydrocarbon.

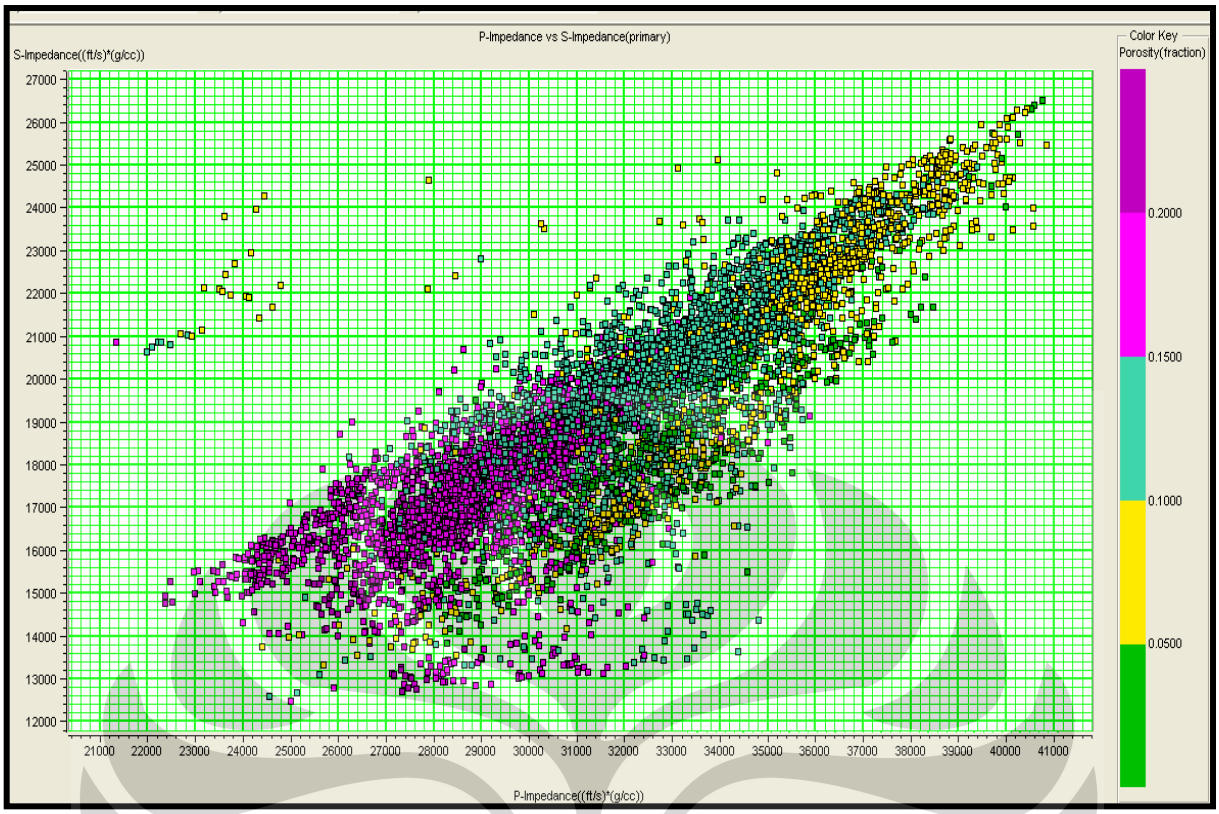

Figure 4.3 Porosity trend on P-impedance vs S-impedance. The porosity tend to be increase when impedance decrease.

The porosity trend acts similarly enough on both P-impedance and S-impedance that the stay tighly clustered within the same trend. Figure 4.4 is a crossplot of P-impedance vs porosity, color coded by water saturation. From this relationship, we can extract an equation to estimate porosity volume from P-impedance volume, as written as follow:

$$\phi = -1.20\text{x}10^{-5}\, P_{impedance} + 0.53 \qquad (4.2)$$

This equation will be used to transform P-impedance volume inverted from seismic data to generate porosity volume. Due to regresion line is superimpose to water saturation value, the porosity transform resulted from this equation is expected to identify fluid content dependent to porosity value. This is complementary technique to map and deliniate pore fluid distribution.

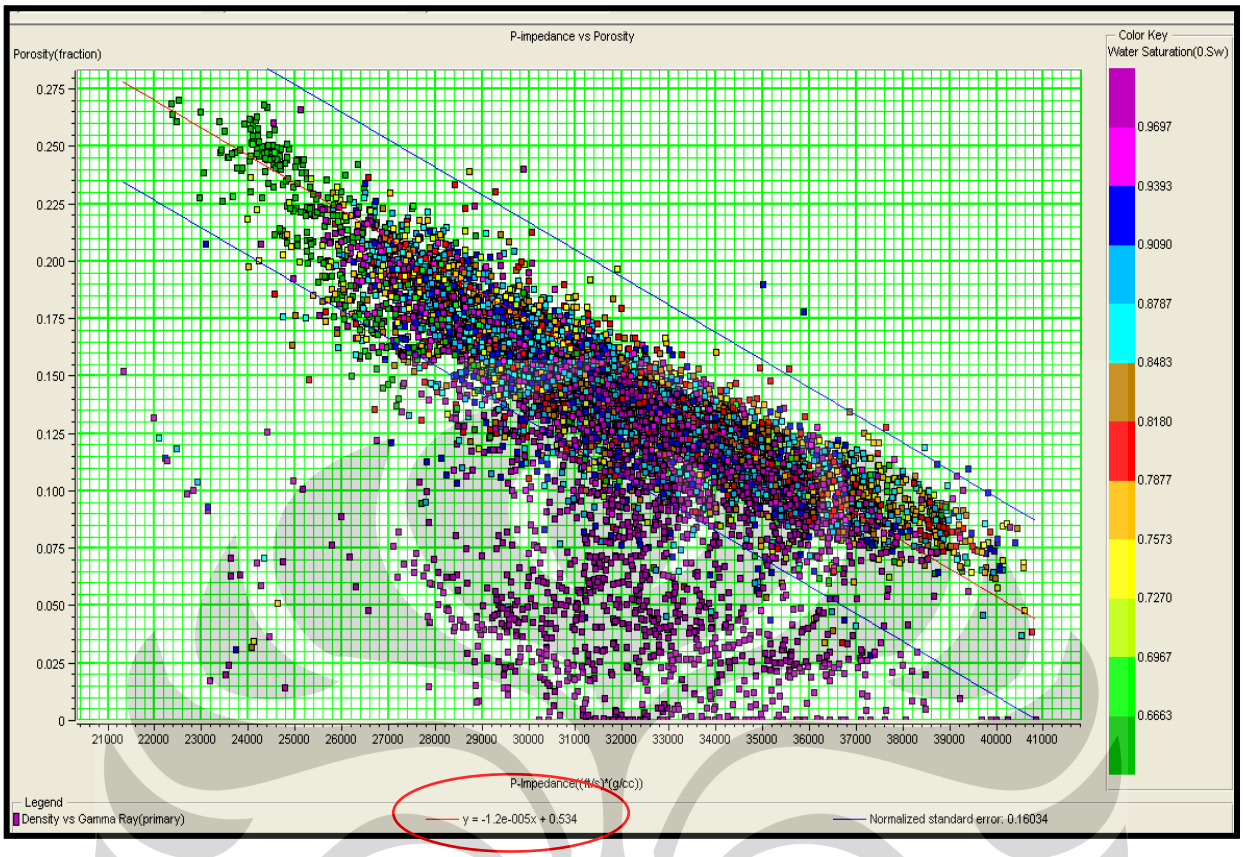

Figure 4.4 P-impedance vs porosity crossplot showing a general trend. A regresion line is made to quantify P-impedance to porosity relationsh

Clay content may affect porosity interpretation based on velocity reading. On this RPT we can see also a high porosity population in shale clustered. This is explained by a data adapted from Marion (1990, courtasey from Avseth et al, 2005) relates porosity and P-wave velocity versus clay content for shaly sands and sandy shales (figure 4.5). Marion introduced a topological model for sand-shale mixtures to predict the interdependence between velocity, porosity and clay content. For shaly sands, it can be assumed that clay particles are strictly located within the sand pore space. Then, total porosity will decrease linearly with increasing clay content. When clay content exceeds the sand porosity, the addition of clay will cause the sand grains to become disconnected, as we go from grain-supported to clay-supported sediments (i.e. shales). Therefore the porosity tend to be increase as clay content increase, effecting decrease of velocity as usual detected on clean sand or shale sand reservoir. This is why in our RPT able to determine porosity on non productive shale.

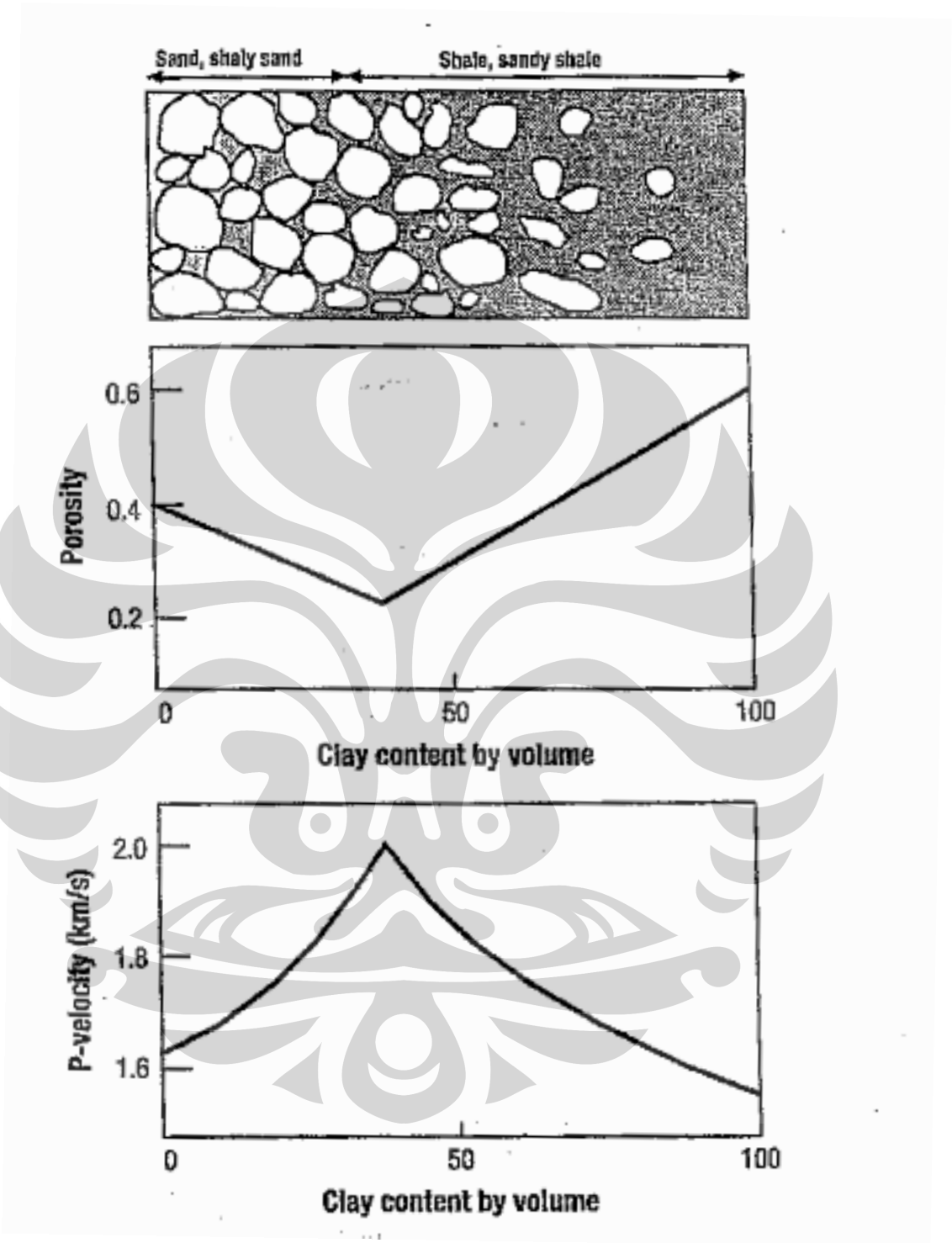

Figure 4.5 Porosity and Vp versus clay content for the porosity minimum and velocity maximum at the transition from grain supported sediment to clay supported sediment (Adapted from Marion, 1990. Courtesy from Avseth et al, 2005)

The big challenge in applying rock physics tools to reservoir chracterization of Menggala fluvial system, is to detect hydrocarbon content and predict its distribution on seismic scale. In Rock Physics Template figure 4.6 show water saturations populations on P-impedaance vs S-impedance crossplot. We cut off Sw 50% as water line so that rock with Sw below 50 % is interpreted as hidrocarbon content. From well testing (DST) at DEFI-01 well we observed the fluid content is gas in high porosity sand. Therefore the low Sw populations on RPT are clustered as gas sand zone. This RPT shows similar interpretability that gas vs water saturated rocks are well separated when impedance are low, which is the sand has high porosity, and poorly separated =when the impedances are high. Also the trend for changes in saturation is essentially perpendicular to the trend for a change in porosity above 15%. This case is similar to the investigation of Avseth et al (2005) and a case from Gulf of Mexico which are referred by this study. Avseth et al compares data from Han (1986), Bargy (1992) and Yin (1992) to separate water and gas saturated sand (figure 4.7). Saturation discriminatios are very similar in different attribute domains, it is poor when porosity is low and good when porosity is high. Moreover, we apply a Biot-Gassman fluid susbtitution method to see further affect of fluid and pore space. As described in chapter 3 section 3.2.1, we substitute initial water saturation to 30% for all Upper and Lower Menggala interval. The predicted result showed that replacing water content to 30% decreases slightly density and P-wave velocity in the Menggala sand, therefore the impedance decreases by about 3%. The less decreases bring forth to porosity substitution to investigate what if the porosity change? Again, by applying Biot-Gassman, now we substitute initial porosity (range 10-18 %) to 5 %. The result showed that decreasing porosity cause large increases density, P-wave velocity and S-wave velocity. This change raises strong presumptions that porosity will lead fluid identification on rock physics parameter both on log scale and seismic examinations.

The remarkable pattern in figure 4.7 is the heart of virtually all direct hidrocarbon detection methods. In spite of many competing parameters that influence velocities, the non fluid effects on Vp and Vs are similar. Variations in porosity, shaliness, and pore pressure move data up and down along the trends, while changes in fluid saturation move data from one trend to another. For reservoir monitoring, the key result is that changes in saturation and changes in pore pressure are nearly perpendicular in the Vp vs Vs crossplot or P-impedance vs S-impedance crossplot.

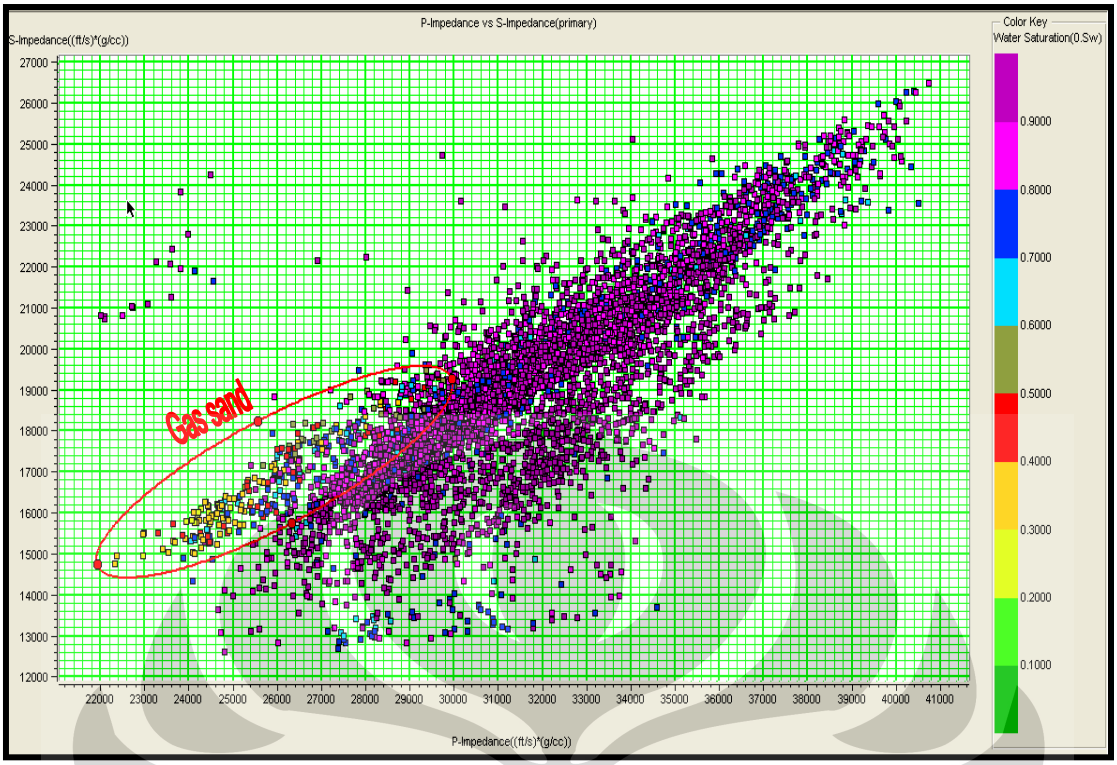

Figure 4.6 Water saturation population on P-impedance vs S-impedance crossplot. The polygon is the gas sand zone, well recognized on low impedance area

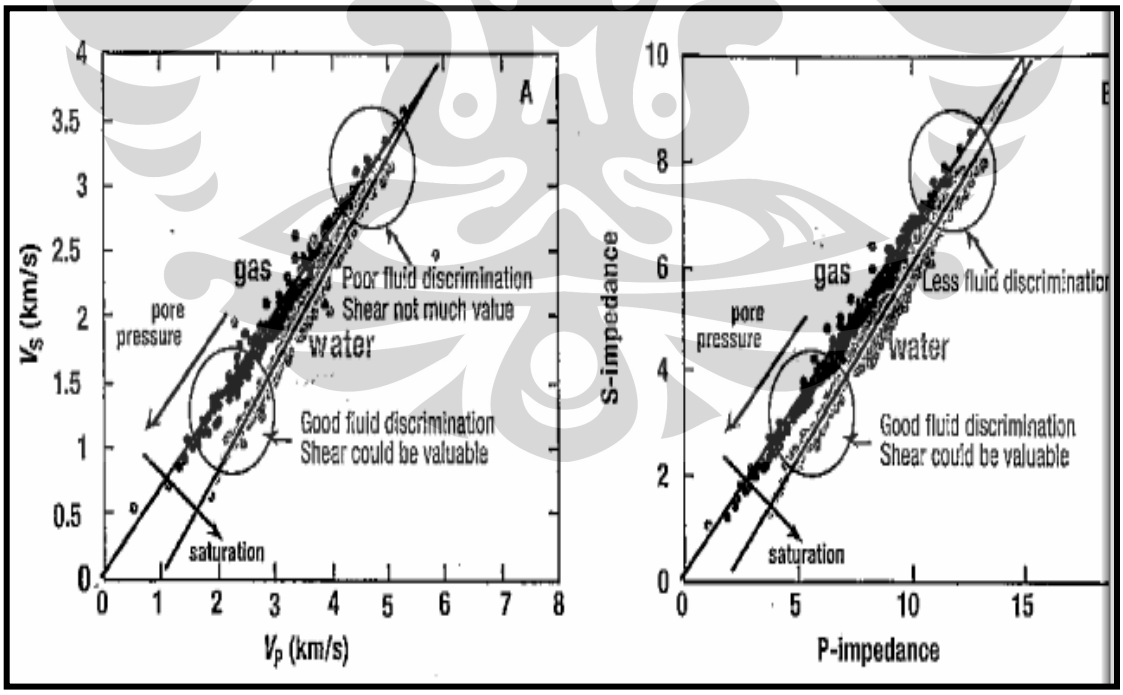

Figure 4.7 Crossplot of Vp vs Vs (left) and P-impedance vs S-impedance (right) on sandstone data. Fluid discrimination is poor when velocity and impedance are low. (Courtesy from Avseth et al, 2005)

Other parameter of rock physics tool which is also valuable for determining hydrocarbon content in Menggala fluvial system is Density (figure 4.8). By RPT density vs Vp/Vs we can see clearly that a low water saturation (<60%) is detected by low density (< 2.3 g/cc). This is gas effect containing in pore space reducing density reading on well log data. Since density parameter can be extracted from seismic data, this qualitative judgment can be useful to predict hydrocarbon on seismic section.

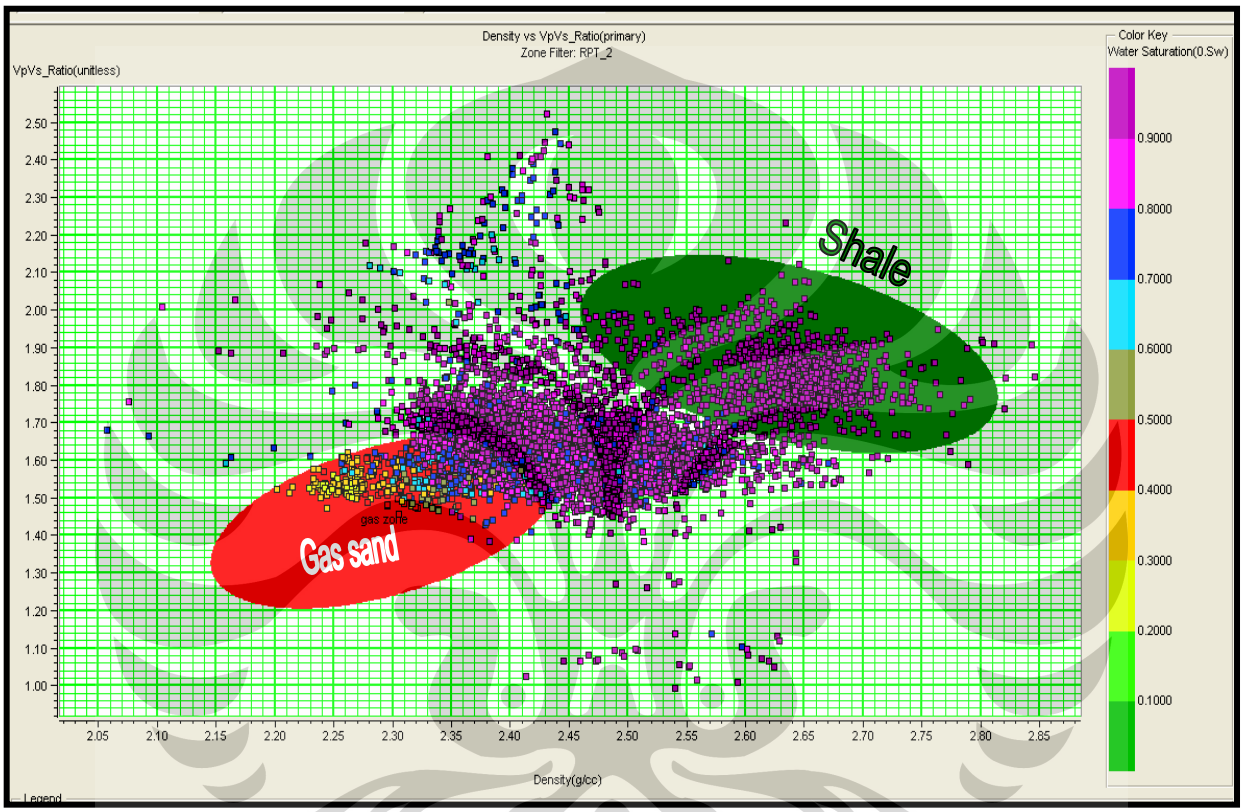

Figure 4.8 Gas zone recognation by color coding density vs Vp/Vs ratio plot with water saturation data. Gas zone (red) tend to be clustered on the right side of 2.3 g/cc density

4.2. Rock physics application to seismic inversion result

Three (3) volume of simultaneous inversion result from partial stacked seismic data exists around the well for rock physics analysis, as described in the study workflow phase 2 (see chapter 3). By Fatti's modification of Aki-Richards equation which was discussed in chapter 2, we calculated reflectivity as a function of Vp, Vs, density and angle, then the information from the data input is calculated a relationship between the four parameters to generate P-impedance model, S-impedance model, and density model. From these models, we can also calculate other rock physics parameter, such as: Vp/Vs, poisson's ratio, Lambda-rho and Mu-rho. But based on rock physics analysis as we processed on well log data, we just generate additional Vp/Vs model to support shale identification. The prior model (initial model) was created by extrapolation of well log data along the defined structural horizons. We used two well defined markers for this purpose: the top Upper Menggala as the top window and top Upper Pematang as bottom window. A different wavelet is used for near, mid and far angle stack inversions based on the amplitude spectrum of a selected window.

Figure 4.9 show vertical sections of inverted P-impedance and S-impedance across the Menggala reservoir. This is crossline section trending relatively north to south. Gamma ray curve from key wells are inserted to see correlation inversion result to well data. Top Upper Menggala and bottom of Lower Menggala horizon are used to delineate inversion window as per study interest. The area outside inversion window is colored by green. We observed low impedance value (P-impedance 28000-29000 ft/s*g/cc and S-impedance 16000-17000 ft/s*g/cc) along cross section through DEFI-09 and tend to increase to the south as detected on DEFI-11 well. Gamma ray curve at both well locations stay same so that we assume the low impedance feature is gas effect as we observed in DEFI-09 well. Porosity changes may also affect to impedance value. Well data indicates that the change is observed laterally and vertically. As discussed previously, Upper Menggala and Lower Menggala has different porosity range where Upper Menggala tend to be cemented or shaly so that its porosity is low. Inverted P-impedance and S-impedance model also indicates low porosity distribution along Upper Menggala section by relatively higher impedance distribution, compared to Lower Menggala section. Laterally, impedance tends to be higher as we go to the south due to low porosity value at the flank of reservoir.

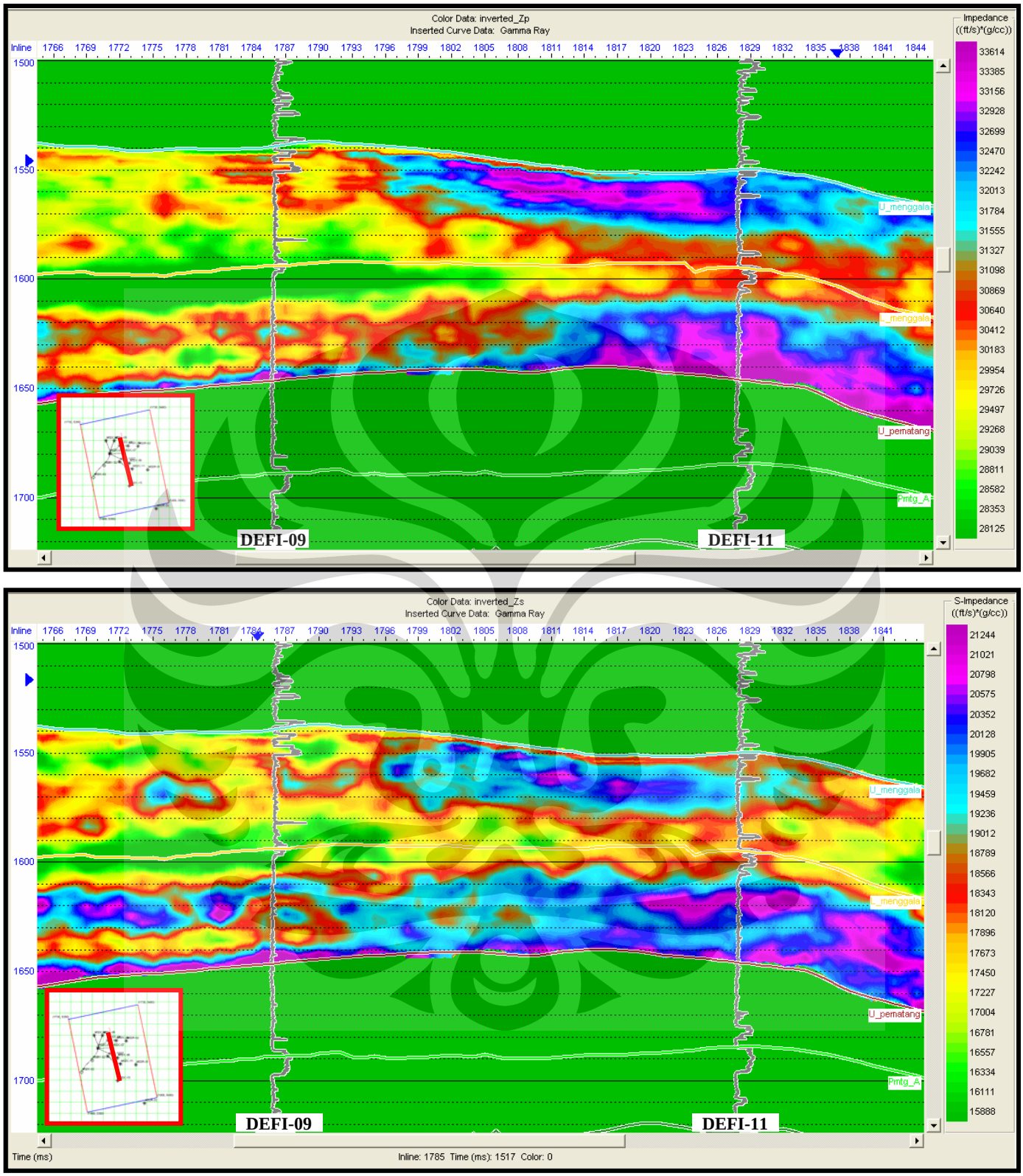

Figure 4.9 Inverted P-impedance (top) and S-impedance (bottom) from seimic data showing lateral distri bution across DEFI-09 to DEFI-11 well (N-S line). A low impedance zone is observed along DEFI-09 well, assumed as gas effect and porosity variations.

Similar to the RPT construction on well log data, we crossplot P-impedance volume versus S-impedance volume from seismic inversion and superimpose to available RPT zone (figure 4.10). The X and Y axis scale is adjusted as same as RPT from well log data to fit the color zone on seismic data. Along crossplot, we can see a significant different of seismic data distribution and well log data populations. Seismic data is more clustered than elongate well log data distributions. Therefore, shaly sand zone which is defined from high impedance area of well log data, unable to reach by seismic data. Seismic impedance is lower than well log impedance both on X and Y axis. However, we can potentially detect gas sand zone and shale zone on seismic scale since these two zones are superimpose to the seismic populations. The data which are excluded on the color zone will be defined as porous sand with high probability to be filled by formation water.

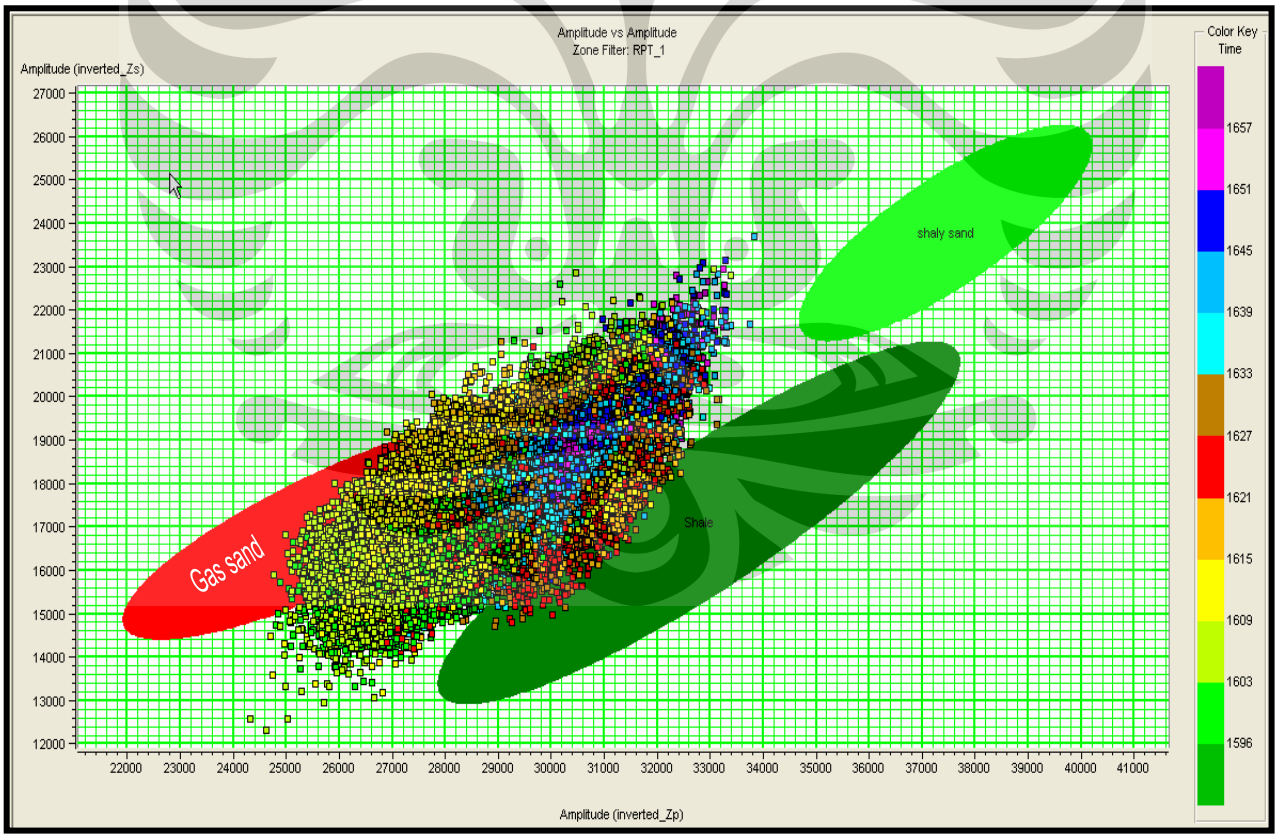

Figure 4.10 Crossplot inverted P-impedance vs S-impedance, overlaid with RPT from well log data. We can potentially detect gas sand and shale dsitributions on seismic scale since the RPT zone fit to seismic data

The color zones are then applied to the seismic section to observe lateral distribution of lithology and pore fluid. In figure 4.11, the gas sand on Upper and Lower Menggala is identified on seismic section through DEFI-10 well in the north with adjacent porous sand to the south. Shale or shaly sand is observed also developing in south area, particularly within Upper Menggala reservoir. RPT from density vs Vp/Vs ratio crossplot is also applied to support shale detection at the level of Menggala window (not displayed). The figure also shows where shale layer identified from seismic is suitable to high GR on well log. A good match of inverted seismic data to the fluid contact identified from well data is observed at DEFI-01 exploration well, where a vertical section of classified RPT match to gas contact depth at DEFI-01 exploration well particularly on Lower Menggala reservoir. Rock physics fail to detect gas content on Upper Menggala section since this reservoir has lower porosity based on petrophysical analysis. The RPT tell us that gas vs water saturations is poorly separated when porosity is low. From DEFI-01 and DEFI-09 well data, Upper Menggala has porosity < 15 % therefore we just observed sand distribution with facies variation to shaly sand within Upper Menggala reservoir

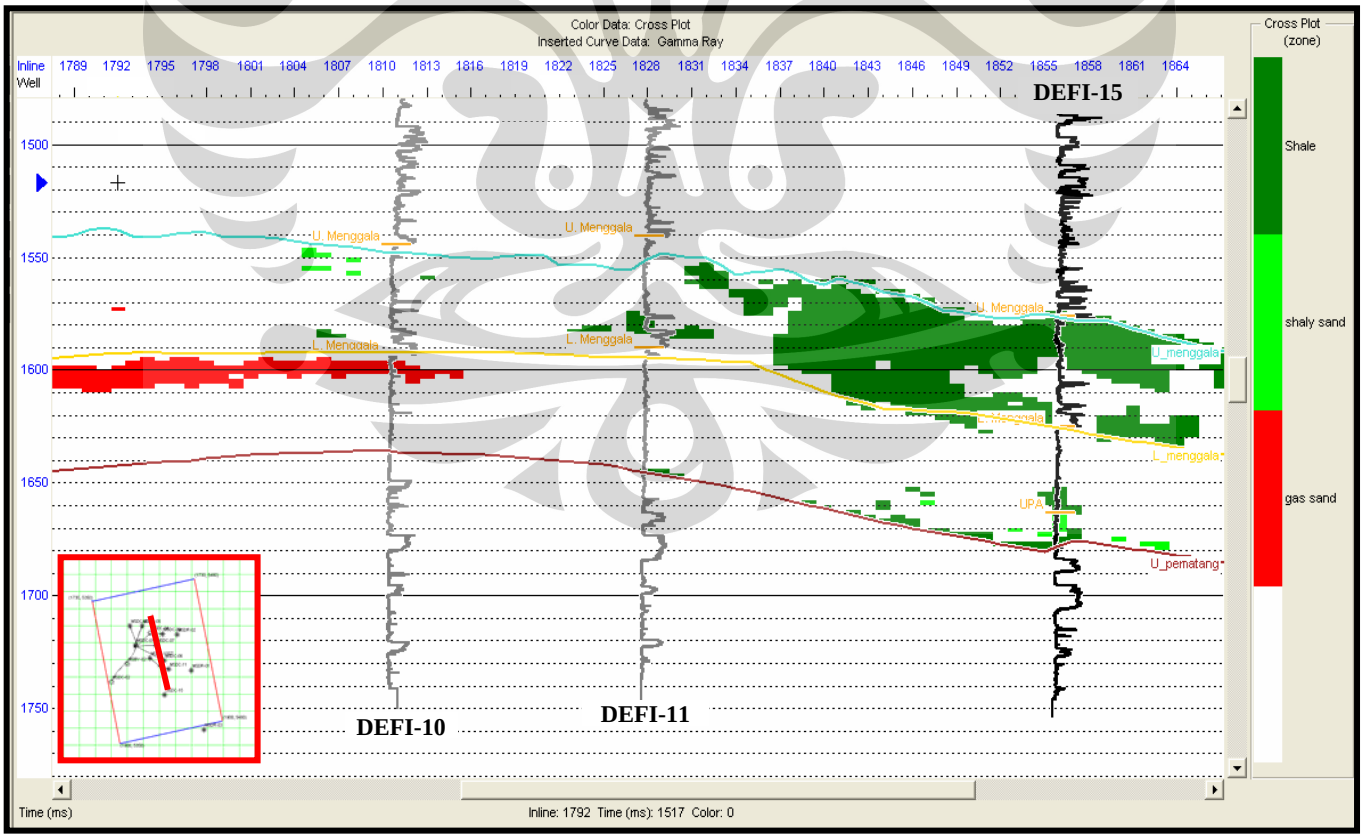

Figure 4.11 vertical section of RPT classified lithofacies across DEFI field. Observed the distribution of gas sand tend to disappear to the south

4.3. Seismic Reservoir Mapping and Near Field Exploration

To display seismic attributes in map view, we have plotted a horizon slice at top of Upper and Lower Menggala (with a window of 15 ms centered) of the inverted seismic volume, color key by RPT classification. This slice is useful for delineating the gas sand and lithology distribution. The resulting map shows lateral distribution of classified lithology and fluid along Upper Menggala and Lower Menggala reservoir (figure 4. 12). These two maps showing contrast distributions where Upper Menggala is dominated by shale (green) and Lower Menggala is dominated by gas sand (red). The white zone on both Upper and Lower Menggala map is zone which is not included in gas sand or shale zone but potentially as porous sand zone. However, porous sand with <15% porosity is not sensitive to fluid change if identified by rock physics parameter. Thus, Upper Menggala is more complicated to expose gas sand distribution since this reservoir is shaly and high cemented, causing decrease of porosity. The further investigation may be elaborated on the white non shaly zone by upscaling proven gas sand from well log data observed on Upper Menggala and then extrapolated to white non shaly sand. A geostatistical or neural network method may be implemented to solve this problem.

A prospect reservoir is easier to be mapped on Lower Menggala level. We identify a rather patchy but channelized outline of gas sand in the south west and north east of the study area which are validated by several drilling well. A shale distribution is also detected on the middle and southeast area (green) as confirmed by DEFI-15 well. The red zone also indicates the higher porous sand than the white zone one. Since almost all drilling wells are penetrated in the northern part of DEFI field, the southwest red zone is potentially to explore by proposed drilling well. The shale facies is almost absent in Lower Menggala level since this reservoir is dominated by blocky massive sand as product of braided channel bar and incised valley fan. However, the thin layer of shale or interbedded of sand-shale facies is potentially failed to be identified due to seismic resolution problem. From sonic log we obtain velocity of reservoir as average 10000 ft/sec and from seismic data we obtain frequency dominant is 20 Hz. So the vertical resolution that we can resolve from seismic data is ¼ λ or 125 ft. The maximum thickness of shale os blow the seismic resolution (10-20 ft)

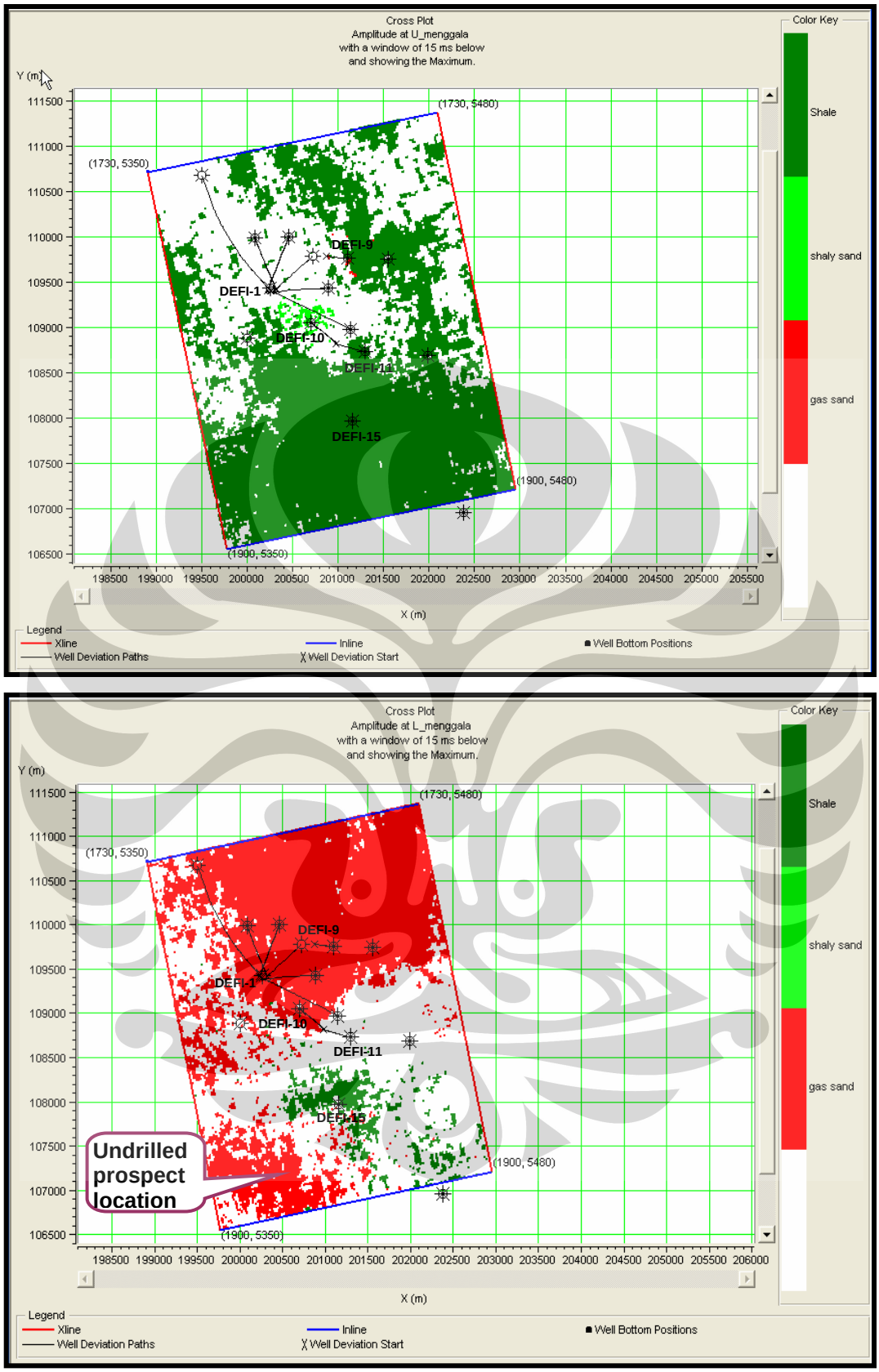

Figure 4.12 Horizon slice map of RPT classified lithofacies at Upper Menggala (top) and Lower Menggala (bottom) showing the deliniation of estimated fluid and lithology

The prospective porous sand distribution based on RPT classification is supported by estimated porosity map which is generated from inverted P-impedance. Since we have equation 4.2 from P-impedance vs porosity relationship, we may estimate porosity distribution along Lower Menggala reservoir (figure 4.13) and the map shows a good match with the lithology and fluid distribution map displayed in figure 4.12

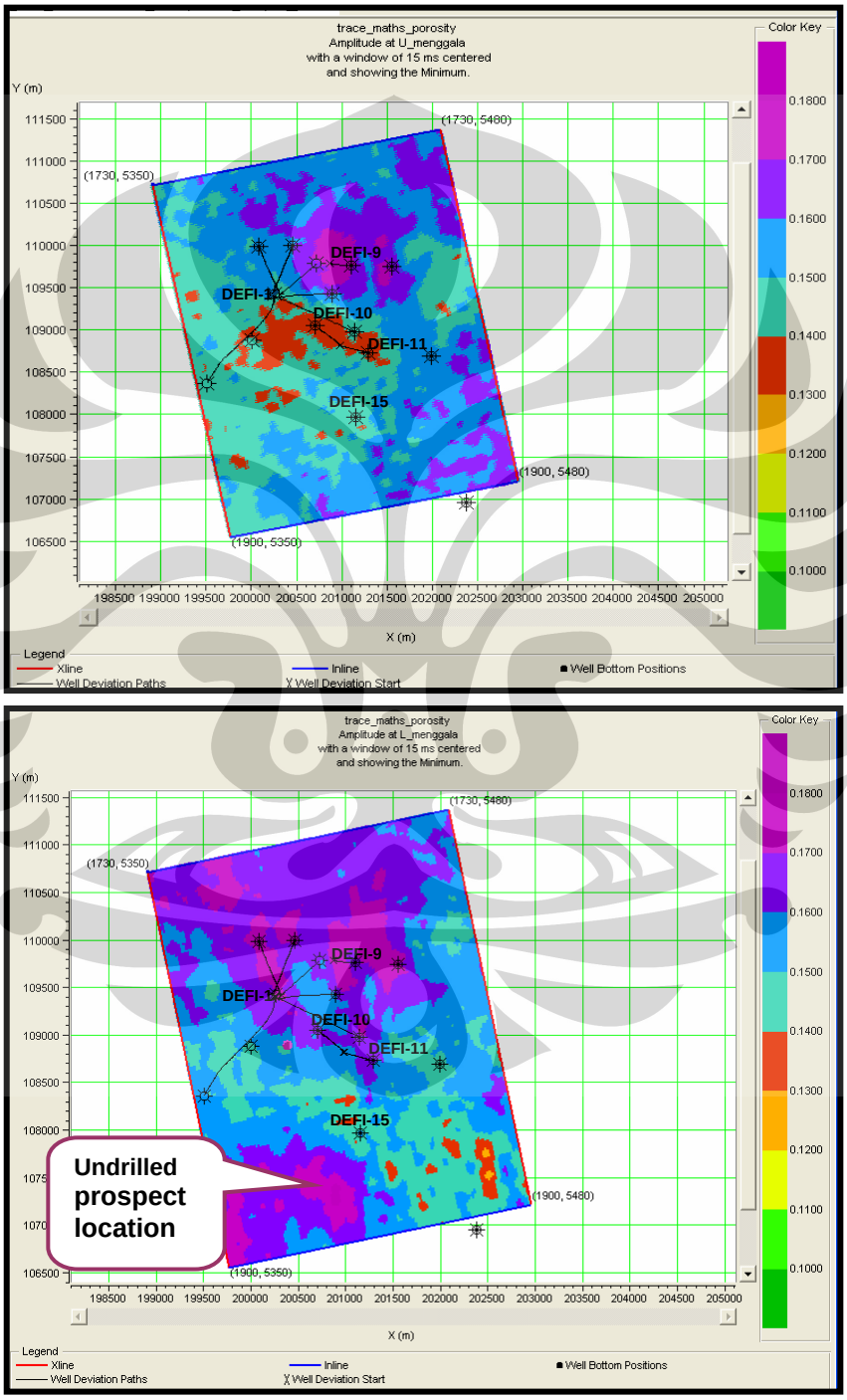

Figure 4.13 Horizon slice map of porosity distibution from inverted P-impedance at Upper Menggala (top) and Lower Menggala (bottom). The prospective porous sands are clustered by light purple zone

In term of near field exploration and drilling prospect generation, we overlay the porosity distribution to Lower Menggala structure map (figure 4.14). Dark purple zone represents the high porous sand with gas-filled potential. The zone is overlaid with closure contours against fault, generating prospect drilling location. Since the north closure area is already proven by some drilling wells and then applied to construct the model, an undrilled prospect location is determined for the southwest area. This two prospect area are possible to have different depositional facies based on regional study. Paradigm (2002) has been performed regional seismic interpretation to identify seismic facies and attribute distribution. Figure 4.15 is courtesy from the project to support regional play concept for our prospect. Those are amplitudes map and seismic facies map showing en-echelon/curvi-liner fault as result of strike-slip deformation in Late Oligocene and curved channel body feature as a product of incised valley fan.

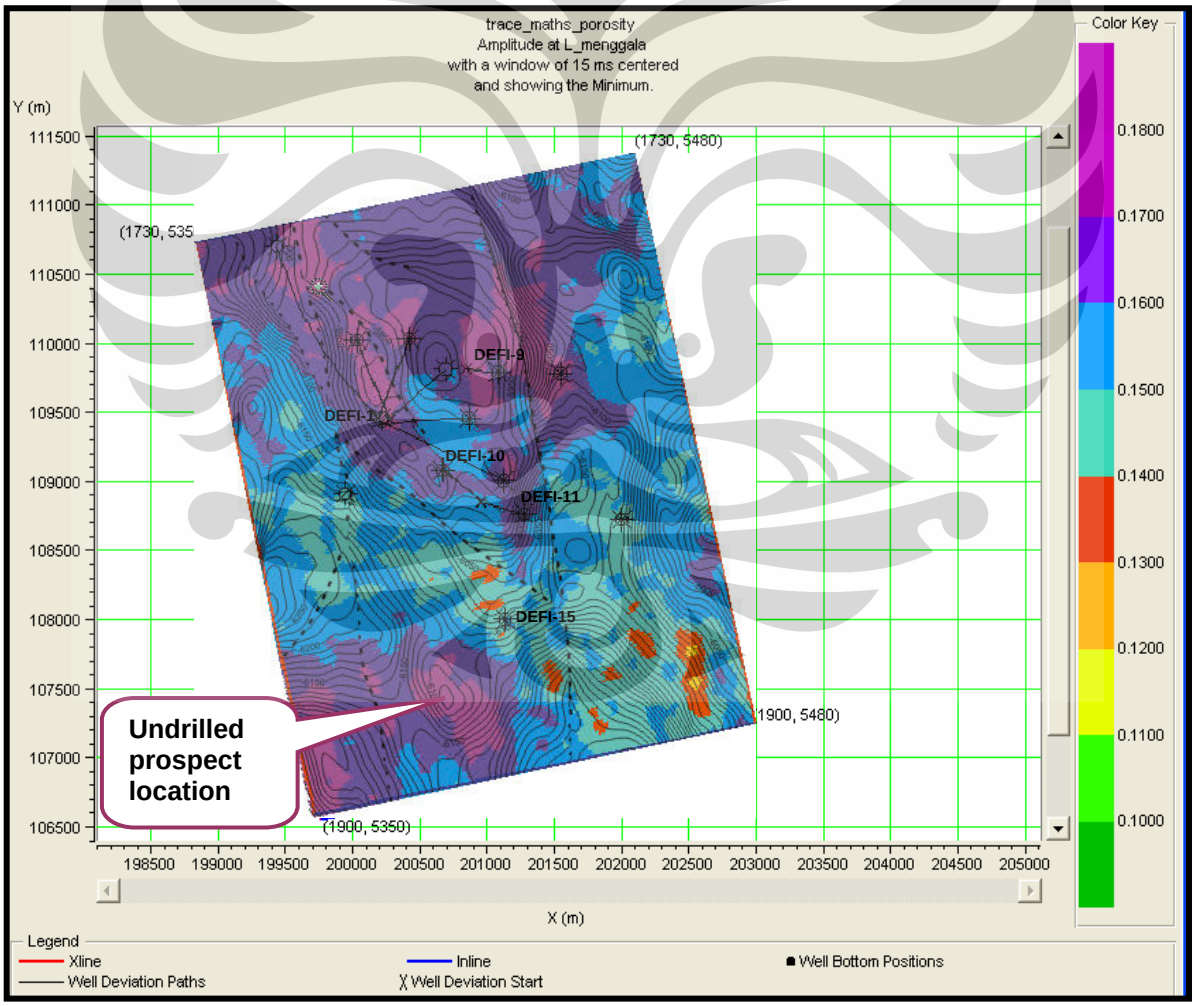

Figure 4.14 Lower Menggala structure map overlaid on porosity map from seismic inversion result. A four way dip closure or against fault is identifed as prospect drilling location

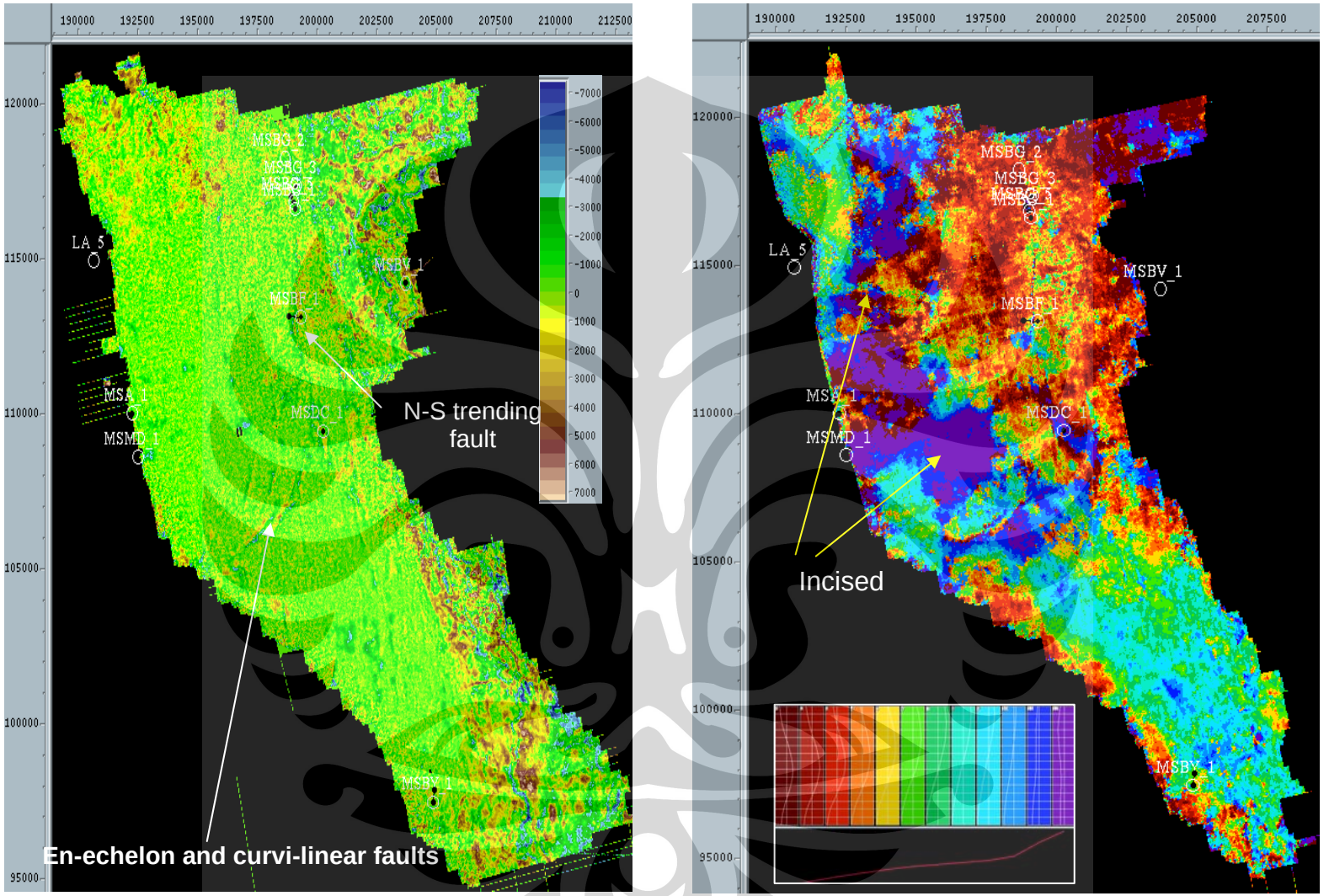

Figure 4.15 Seismic amplitude anomaly showing structural trend recognized on Lower Menggala (Left). Regional seismic facies map based on waveform classification showing indication of incised valley fan morphology on Lower Menggala time (right)

Chapter Five:
CONCLUSIONS AND RECOMENDATIONS

We have demonstrated how Rock physics analysis can be used to guide interpretation and delineate lithology and reservoir properties distribution in the DEFI field. The methodology consists of two phase: selecting the rock physics template that is consistent with the well log data and applying the user defined Rock Physics template to characterize reservoir distribution in the seismic data. This is a semi-quantitative method. The templates are based on quantitative rock physics model, but the validation with log data, and especially the choice of separation polygons is based on qualitative judgement.

The result shows that we can potentially distinguish rock physics of Upper Menggala and Lower Menggala reservoir through well log data. Reservoir Porosity has a similar trend and closest relationship to acoustic dan elastic parameter while fluid discrimination is detectable only for reservoir above 15 % of porosity; in this case Upper Menggala reservoir is more difficult to recognize the hydrocarbon distribution due to low porosity. We are also able to delineate the porous gas sands reservoir distribution through seismic data based on rock physics template which is validated from well log data. Finally, a prospective undrilled area is generated based on reservoir distribution map characterized by rock physics tool.

Therefore we recommend the prospect drilling location in the southwestern of DEFI field to validate Menggala reservoir characterization and distribution. The validation of Rock physics analysis is required as input in near field exploration and development during the production phase of the DEFI field particularly for the deeper target or other prospective reservoir. A further rock physics-based study may be implemented to neighbor field to expand Menggala reservoir exploration outside DEFI field.

REFERENCES

Avseth P, Mukerji T., & Mavko G., 2005. **Quantitative Seismic Interpretation, Applying Rock Physics Tools to Reduce Interpretation Risk**. Cambridge University Press. UK

Bactiar A., Juber F., Soenoro A., Saputra S., Irawan C., **Menggala Exploration and Production Strategy – Bengkalis Through Malacca Strait PSC,** Internal report for Kondur Petroleum SA, Unpublished

Chi, X.G., & Han, D.H., 2009. **Lithology And Fluid Differentiation Using A Rock Physics Template**. The Leading Edge, January 2009

Connolly, P., 1999. **Elastic Impedance**, The Leading Edge, p.438-453

DC Development Team. 2008. **DC/Kuat Drilling Proposal**. Kondur Petroleum Internal Report. Unpublished

Gautama Y., Gustiawan E., 2001. **Petroleum Engineering Study of Menggala,** Internal report for Kondur Petroleum SA, Unpublished

Lambiase, J., 1997. **Syn-Rift Stratigraphic Study of the Bengkalis and Padang Troughs – Malacca Strait PSC,** Internal report for Kondur Petroleum SA, Unpublished

Ma, X.Q., 2002. **Simultaneous inversion of prestack seismic data for rock properties using simulated annealing**, Geophysiscs, 67, p. 1877-1885

Morris, H.J.S., et al. 2008. **Fast Track Reservoir Characterization of A Subtle Paleocene Deep marine Turbidite Field Using A Rock Physics And Seismic Modelling led Workflow**. 32nd IPA Annual Convention & Exhibition. Jakarta.

Munadi, Suprayitno, 2005, **Prinsip Inversi Seismik**, Lembaran Publikasi Migas vol. 39 No.1. Jakarta

Pennington, W.D., 2008. **Advanced Seismic Petrophysics**. NEXT Course Note. Bandung

Sunjaya, E.S., 2002. **Transition to Menggala Study Volume 1**, Kondur Petroleum Internal Report. Unpublished